

GLAST

Exploring Nature's Highest Energy
Processes with the Gamma-ray
Large Area Space Telescope

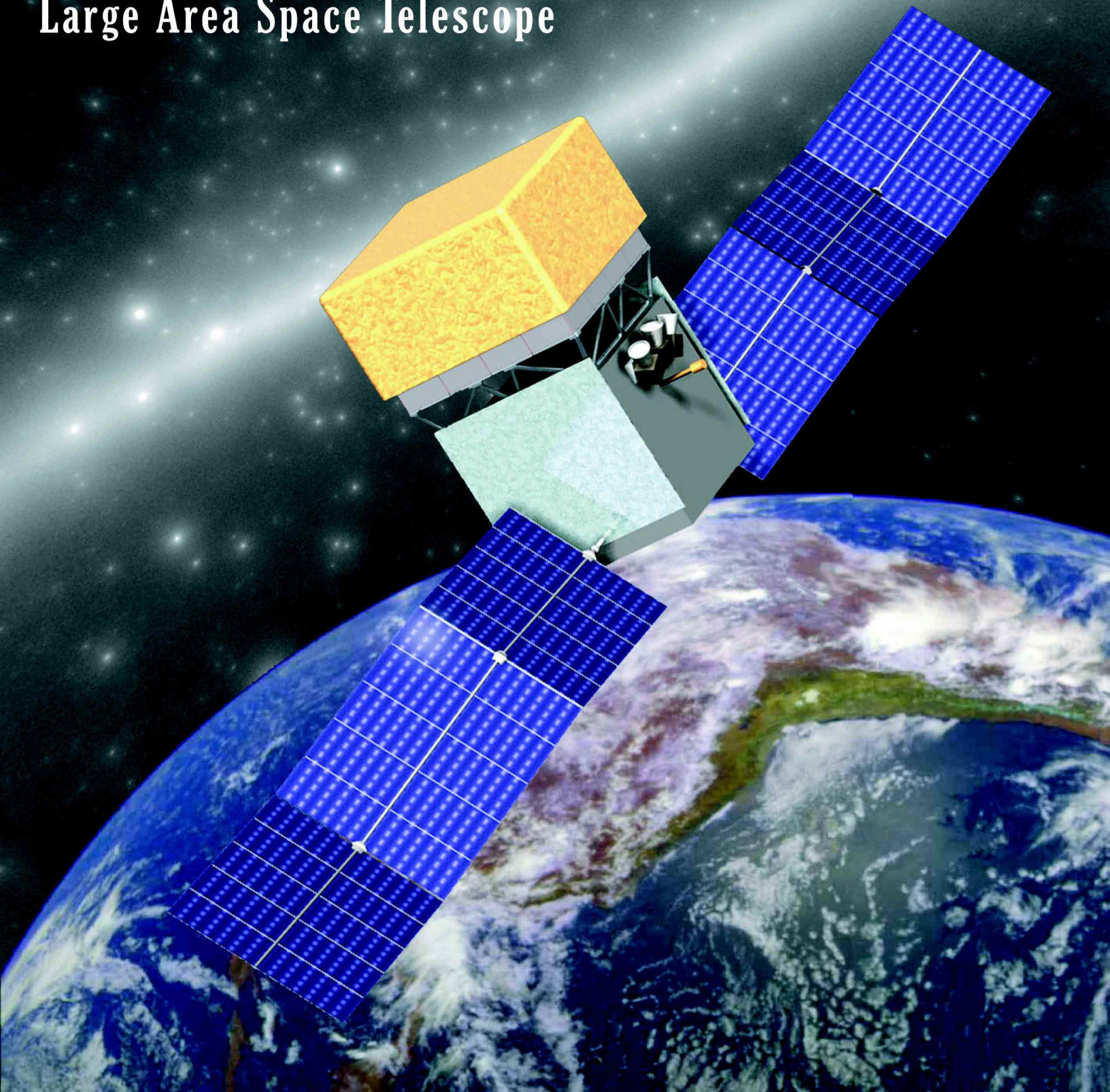


Table of Contents

1. EXECUTIVE SUMMARY	3
2. INTRODUCTION	6
3. BLAZARS AND ACTIVE GALACTIC NUCLEI	8
3.1 BLAZAR MODELS	
3.2 AGN OBSERVATIONS WITH GLAST	
3.3 BLAZAR COSMOLOGY WITH GLAST	
4. UNIDENTIFIED SOURCES	13
4.1 GLAST OBSERVATIONS OF UNIDENTIFIED SOURCES	
4.2 POTENTIAL NEW SOURCE CLASSES	
5. COSMOLOGY AND THE DIFFUSE BACKGROUND	15
5.1 DEEP SURVEY OF DIFFUSE BACKGROUND FOR SIGNATURES OF UNSTABLE PARTICLE RELICS	
5.2 GAMMA-RAY LINES FROM SUPERSYMMETRIC PARTICLE DARK MATTER ANNIHILATION	
6. GAMMA-RAY BURSTS	18
6.1 HIGH-ENERGY EMISSION AND GRB MODELS	
6.2 HIGH-ENERGY GRB OBSERVATIONS AND ASTROPARTICLE PHYSICS	
6.3 EXPECTED GLAST OBSERVATIONS OF GRBS	
7. PULSARS	22
7.1 GAMMA-RAY OBSERVATIONS	
7.2 GLAST AND PULSAR MODELS	
8. COSMIC RAYS AND INTERSTELLAR EMISSION	24
8.1 RECENT RESULTS	
8.2 ADVANCES WITH GLAST	
9. SOLAR FLARES	28
9.1 EGRET OBSERVATIONS	
9.2 CONTRIBUTIONS FROM GLAST	
10. COMPLEMENTARITY WITH GROUND-BASED EXPERIMENTS	30
11. INSTRUMENT DEVELOPMENT	32
11.1 LARGE AREA TELESCOPE	
11.2 GLAST BURST MONITOR	
12. MISSION OVERVIEW	34
12.1 OPERATIONS	
12.2 DEVELOPMENT SCHEDULE	
12.3 ORGANIZATION	
12.4 LAUNCH VEHICLE AND SPACECRAFT	
REFERENCES	36
FIGURE CREDITS	38
CONTRIBUTORS TO THIS DOCUMENT	38

1. Executive Summary

The **Gamma-ray Large Area Space Telescope** (GLAST) is an international space mission that will study the cosmos in the energy range 10 keV–300 GeV, the upper end of which is one of the last poorly observed regions of the celestial electromagnetic spectrum to be explored. Several successful exploratory missions in gamma-ray astronomy led to the Energetic Gamma Ray Experiment Telescope (EGRET) instrument on the Compton Gamma Ray Observatory (CGRO). Launched in 1991, EGRET made the first complete survey of the sky in the 30 MeV–10 GeV range. EGRET showed the high-energy gamma-ray sky to be surprisingly dynamic and diverse, with sources ranging from the Sun and Moon to massive black holes at large redshifts. Most of the gamma-ray sources detected by EGRET remain unidentified. EGRET uncovered the tip of the iceberg, raising many questions, and it is in the light of EGRET’s results that the great potential of the next generation gamma-ray telescope can be appreciated.

GLAST will have an imaging gamma-ray telescope vastly more capable than instruments flown previously, as well as a secondary instrument to augment the study of gamma-ray bursts. The main instrument, the Large Area Telescope (LAT), will have superior area, angular resolution, field of view, and dead time that together

will provide a factor of 30 or more advance in sensitivity, and capability for study of transient phenomena (Table 1-1). The GLAST Burst Monitor (GBM) will have a field of view several times larger than the LAT and will provide spectral coverage of gamma-ray bursts that extends from the lower limit of the LAT down to a few keV. The basic parameters of the GBM are compared to those of the Burst and Transient Source Experiment (BATSE) instrument on CGRO in Table 1-2. With the LAT and GBM, GLAST will be a flexible observatory for investigating the great range of astrophysical phenomena best studied in high-energy gamma rays. NASA plans to launch GLAST in late 2005.

The anticipated advances in astronomy and high-energy physics with GLAST are described briefly below. They are among the central subjects of NASA’s Structure and Evolution of the Universe (SEU) research theme and the Department of Energy’s non-accelerator research program. The GLAST mission is also supported by the physics and astrophysics programs in the partner countries of France, Germany, Italy, Japan, and Sweden. NASA recognizes the scientific goals of the GLAST mission as part of the SEU Cosmic Journeys planned for study of black holes and dark matter. Of course, with its capabilities, GLAST

Table 1-1 GLAST LAT Specifications and Performance Compared with EGRET.

Quantity	EGRET	LAT (Minimum Spec.)
Energy Range	20 MeV – 30 GeV	20 MeV – 300 GeV
Peak Effective Area¹	1500 cm ²	8000 cm ²
Field of View	0.5 sr	>2 sr
Angular Resolution²	5.8° (100 MeV)	<3.5° (100 MeV) <0.15° (>10 GeV)
Energy Resolution³	10%	10%
Deadtime per Event	100 ms	<100 μs
Source Location Determination⁴	15′	<0.5′
Point Source Sensitivity⁵	$\sim 1 \times 10^{-7} \text{ cm}^{-2} \text{ s}^{-1}$	$< 6 \times 10^{-9} \text{ cm}^{-2} \text{ s}^{-1}$

¹ After background rejection

² Single photon, 68% containment, on-axis

³ 1-σ, on-axis

⁴ 1-σ radius, flux $10^{-7} \text{ cm}^{-2} \text{ s}^{-1}$ (>100 MeV), high $|b|$

⁵ >100 MeV, at high $|b|$, for exposure of one-year all sky survey

Table 1-2 GLAST GBM Specifications and Performance Compared with BATSE.

Quantity	BATSE	GBM (Minimum Spec.)
Energy Range	25 keV – 10 MeV	<10 keV – >25 MeV
Field of View	4π sr	all sky not occulted by Earth
Energy Resolution ¹	<10%	<15%
Deadtime per Event		<15 μ s
Burst Sensitivity ²	$0.2 \text{ cm}^{-2} \text{ s}^{-1}$	$<0.5 \text{ cm}^{-2} \text{ s}^{-1}$
GRB Alert Location ³	$\sim 25^\circ$	<15 $^\circ$
GRB Final Location ³	1.7 $^\circ$	<1.5 $^\circ$

¹ 1- σ , 0.1–1 MeV

² 50–300 keV

³ Calculated onboard, 1- σ radius, for a burst of brightness $10 \text{ cm}^{-2} \text{ s}^{-1}$ in 50–300 keV band and duration of 1 s

certainly may yield important unanticipated findings. The mission will be supported by a vigorous, multidisciplinary guest investigator program to maximize the discovery potential.

The Scientific Case for GLAST

The universe is largely transparent to gamma rays in the energy range of GLAST. Energetic sources near the edge of the visible universe can be detected by the light of their gamma rays. There is good reason to expect that GLAST will see known classes of sources to redshifts of 5, or even greater if the sources existed at earlier times. The small interaction cross section for gamma rays also means that gamma rays can provide a direct view into nature’s highest-energy acceleration processes. Gamma rays point back to their sources, unlike high-energy cosmic rays, which are deflected by magnetic fields.

Blazars and Active Galactic Nuclei

EGRET discovered that blazar-class active galactic nuclei (AGNs) are bright and variable sources of high-energy gamma rays. In fact, the bulk of the luminosity for many blazars is emitted in GLAST’s energy range. The emission is believed to be powered by accretion onto supermassive black holes at the cores of distant galaxies. GLAST will increase the number of known AGN gamma-ray sources from about 70 to thousands. Moreover, it will effectively be an all-sky monitor for AGN flares, scanning the full sky every three hours. It

will greatly decrease the minimum time scale for detection of variability, and will offer near-real-time alerts for spacecraft and ground-based observatories operating at other wavelengths. Using EGRET, AGN flares were measured to vary on the shortest time scales – eight hours – that were able to be determined with statistical significance.

Unidentified Sources

GLAST will enable identification of the EGRET sources for which no counterparts are known at other wavelengths by providing much finer error boxes. More than 60% of the EGRET sources are unidentified. Considering their distribution on the sky, less than one third of these are extragalactic (probably blazar AGNs), with the rest most likely within the Milky Way. Recent work suggests that many of these unidentified sources are associated with the nearby Gould Belt of star-forming regions that surrounds the solar neighborhood. Apparently-steady sources are likely to be radio-quiet pulsars – and again, GLAST will be able to directly search for periods in sources at least down to EGRET’s flux limit. Transient sources within the Milky Way are poorly understood, and may represent interactions of individual pulsars or neutron star binaries with the ambient interstellar medium. Some of the unidentified EGRET sources may be associated with recently discovered Galactic microquasars. GLAST will be able to explore these source classes in detail.

New Particle Physics

The large area and low instrumental background of GLAST will also allow searches for decays of exotic particles in the early universe and for annihilations of postulated weakly-interacting massive particles (WIMPs) in the halo of the Milky Way. Much of the isotropic background detected by EGRET will be resolved by GLAST into discrete AGN sources. A truly diffuse, cosmic residual would be a tremendous discovery and could relate to particle decay in the early universe. Recent theoretical work suggests that annihilation emission from the lightest supersymmetric particle, a candidate Galactic halo WIMP, could be detectable with GLAST. The signature would be spatially diffuse, narrow line emission peaked toward the Galactic center.

Extragalactic Background Light

The sensitivity of GLAST at high energies will also permit study of the extragalactic background light by measurement of the attenuation of AGN spectra at high energies. This attenuation is from pair production with photons in the background light primarily produced by young stars at visible to ultraviolet wavelengths. Owing to the large size of the AGN catalog that GLAST will amass, intrinsic spectra of AGNs will be distinguishable from the effects of attenuation. The measured attenuation as a function of AGN redshift will relate directly to the star formation history of the universe.

Gamma-Ray Bursts

GLAST will continue the recent revolution of gamma-ray burst (GRB) understanding by measuring spectra from keV to GeV energies and by tracking afterglows. With its high-energy response and very short deadtime, GLAST will offer unique capabilities for the high-energy study of bursts that will not be superseded by any planned mission. GLAST will make definitive measurements of the high-energy behavior of bursts that EGRET could not. Time-resolved spectral measurements with GLAST, combining data from LAT and GBM, will permit determination of the minimum Lorentz factors and baryon fractions for the emitting regions, and distinguish between internal and external shocks as the mechanism for gamma-ray production, and may also permit gamma-ray-only distance determinations. The LAT and the GBM will detect more than 200 bursts per year and provide near-real-time location information to other observatories for afterglow searches. GLAST will have the capability

to slew autonomously toward bursts to monitor for delayed emission with the LAT.

Pulsars

GLAST will discover many gamma-ray pulsars, potentially 250 or more, and will provide definitive spectral measurements that will distinguish between the two primary models proposed to explain particle acceleration and gamma-ray generation: the outer gap and polar cap models. From observations made with gamma ray experiments through the EGRET era, seven gamma-ray pulsars are known. GLAST will be able to directly search for periodicities in all EGRET unidentified sources. Because the gamma-ray beams of pulsars are apparently broader than their radio beams, many radio-quiet, Geminga-like pulsars likely remain to be discovered.

Cosmic Rays and Interstellar Emission

GLAST will spatially resolve remnants and precisely measure their spectra, and may determine whether supernova remnants are sources of cosmic-ray nuclei. Cosmic rays produce the pervasive diffuse gamma-ray emission in the Milky Way via their collisions with interstellar nuclei and photons. GLAST will also be able to detect the diffuse emission from a number of local group and starburst galaxies, and to map the emission within the largest of these for the first time. Spatial and spectral studies of the gamma-ray emission will permit the distributions of cosmic-ray protons and electrons to be measured separately and will test cosmic-ray production and diffusion theories.

Solar Flares

GLAST will have unique high-energy capability for study of solar flares. EGRET discovered that the sun is a source of GeV gamma rays. GLAST will be able to determine where the acceleration takes place, and whether protons are accelerated along with the electrons. The large effective area and small deadtime of GLAST will enable the required detailed studies of spectral evolution and localization of flares. GLAST will be the only mission observing high-energy photons from solar flares during Cycle 24.

Complementarity with Ground-Based Gamma-Ray Telescopes

GLAST in orbit will complement the capabilities of the next-generation atmospheric Cherenkov and shower gamma-ray telescopes that are planned, under construction, or beginning operation, such as CANGAROO III, CELESTE, HESS, MAGIC, MILAGRO, STACEE, and VERITAS. The ground-based telescopes detect the Cherenkov light or air-shower particles from cascading interactions of very high-energy gamma rays in the upper atmosphere. They have very large effective collecting areas ($>10^8$ cm²), but small fields of view ($\sim 1^\circ$, with the exception of MILAGRO) and limited duty cycles relative to GLAST. The next-generation Cherenkov telescopes will have sensitivities extending down to 50 GeV and below, providing a broad useful range of overlap with GLAST.

Because of its unique capabilities and the great increment in sensitivity it offers in a largely unexplored region of the electromagnetic spectrum, GLAST draws the interest of several scientific communities. The international high-energy astrophysics and high-energy particle physics communities together have been particularly active in developing the mission and the necessary technologies.

2. Introduction

One of the last bands of the electromagnetic spectrum to be exploited for astronomy is the range above 20 MeV. The principal reason for the late start was technological: for energies up to tens of GeV, detectors must be placed in orbit, and even from orbit the detection of the low fluxes of celestial gamma rays is difficult. Almost as important is that the range of sources and phenomena, which can be studied in high-energy gamma rays is much broader than had been widely anticipated.

The high-energy gamma-ray sky has been studied with only a few groundbreaking missions. In 1967, an instrument on NASA's OSO III, with an effective area of approximately 4 cm², detected the Milky Way as a source of diffuse gamma-ray emission. SAS-2, launched by NASA in 1972, had an effective area of about 100 cm² and very low instrumental background. Although it operated for only six months, it was the first to detect the isotropic, apparently extragalactic gamma-ray emission. It also detected the Crab and Vela pulsars, and the then-unidentified Geminga pulsar. COS-B, which was launched by ESA in 1975, had an

Instrument Design

The instruments on the GLAST mission are the Large Area Telescope (LAT, principal investigator Peter Michelson, Stanford University) and the GLAST Burst Monitor (GBM, principal investigator Charles Meegan, MSFC, co-PI Giselher Lichti, Max-Planck-Institut für extraterrestrische Physik, Germany). The LAT will have three subsystems: a solid state detector (silicon strip) pair conversion tracker for gamma-ray detection and direction measurement, a CsI calorimeter for measurement of the energies, and a plastic scintillator anticoincidence system to provide rejection of signals from the intense background of charged particles. The LAT will be modular, consisting of a 4×4 array of identical towers, and will have more than 1 million silicon-strip detector channels. The GBM will have twelve NaI scintillators and two BGO scintillators mounted on the sides of the spacecraft. The combined detectors will view the entire sky not occulted by the earth, with energy coverage from a few keV to 30 MeV, overlapping with the lower energy limit of the LAT and with the range of GRB detectors on previous missions.

effective area of about 50 cm² and greater background, owing partly to an elliptical orbit that carried it out of the magnetosphere for most of the time, but it operated for seven years. COS-B observations yielded a catalog of 25 gamma-ray point sources, including 3C 273, the first known extragalactic source. (Some of the sources have since been shown to be diffuse emission unresolved by COS-B.) The Energetic Gamma Ray Experiment Telescope (EGRET) instrument on NASA's Compton Gamma-Ray Observatory (CGRO), which operated from 1991 April until 2000 May, had an effective area of approximately 1500 cm², better angular resolution, a broader energy range, and low instrumental background.

EGRET made the first complete survey of the high-energy gamma-ray sky (Fig. 2-1). The most recent catalog of EGRET point sources has 271 entries. Seven gamma-ray pulsars have been detected in EGRET data, and EGRET observations have established blazars as a class of extragalactic gamma-ray emitters. The majority of the EGRET sources remains unidentified. Many of the sources are variable, like blazars, occasionally

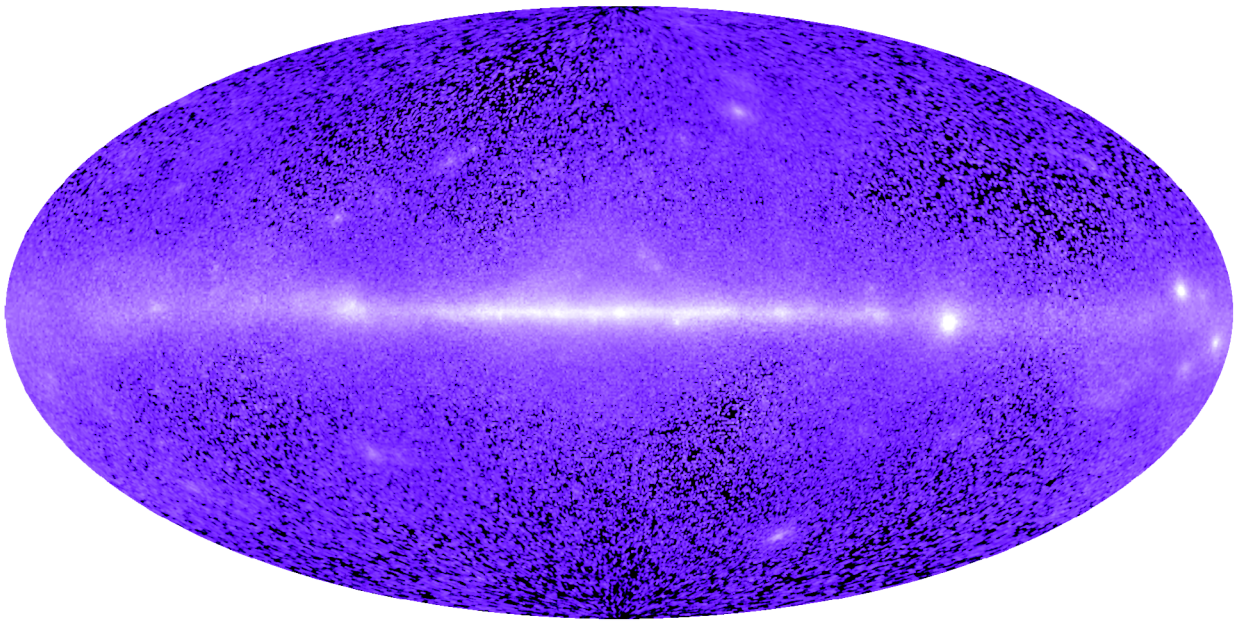


Figure 2-1 EGRET all-sky map in Galactic coordinates for energies greater than 100 MeV. The broad band across the center of the image is diffuse emission from cosmic-ray interactions in the Milky Way. The brightest sources close to the plane are gamma-ray pulsars. The bright sources away from the plane are active galactic nuclei or not yet identified.

flaring on time scales of less than one day. A subset of the steady sources has recently been proposed to be associated with nearby star-forming regions. EGRET also detected high-energy gamma-ray emission from several gamma-ray bursts and from solar flares. The EGRET observations of the Magellanic Clouds established that cosmic rays with energies below the knee of the cosmic ray spectrum are galactic in origin.

The GLAST mission was conceived to address important outstanding questions in high-energy astrophysics, many of which are raised but not answered by results from EGRET. The sections that follow detail the scientific motivations for GLAST: the wide range of effects from nonthermal processes that can best be studied in high-energy gamma rays, from solar flares, to pulsars and cosmic rays in our Galaxy, to active galactic nuclei and gamma-ray bursts at high redshifts. The potential of this energy range for science has only begun to be developed.

This document also includes descriptions of the main instrument on GLAST, the Large Area Telescope (LAT), and a context instrument, the GLAST Burst Monitor (GBM), selected by NASA to augment the study of gamma-ray bursts. The LAT is a pair conversion telescope, like EGRET and its predecessors (Fig. 2-2 and §11), but the detectors will be based on solid-state technology, obviating the need for consumables and greatly decreasing instrument

deadtime. The GBM will extend the spectral coverage of GRBs down to a few keV, to overlap with the large GRB database of other missions, and will increase the fraction of the sky that can be monitored for bursts. Tables 1-1 and 1-2 compare the specifications of the LAT and GBM with EGRET and BATSE (the Burst and Transient Source Experiment on CGRO). GLAST is planned for launch in 2005 (§12).

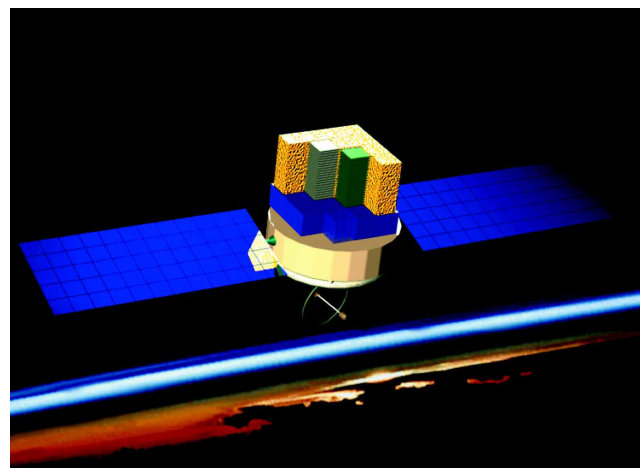


Figure 2-2 An instrument/spacecraft concept for GLAST (see §11 & 12). Some towers and part of the LAT calorimeter have been removed in this cutaway view.

3. Blazars and Active Galactic Nuclei

High-energy gamma rays from 3C 273 were first detected in 1976 with COS-B (Swanenburg et al. 1978). Although predictions of gamma-ray emission from AGNs were made in the interim (Bignami et al. 1979; Königl 1981), the discovery of the gamma-ray blazar class with EGRET (Hartman et al. 1992) was unexpected. Blazar AGNs now compose the largest fraction of identified gamma-ray sources in the EGRET range, with 66 high-confidence and 27 lower-confidence identifications (Hartman et al. 1999). For a blazar, the power in >100 MeV radiation is a significant fraction of the bolometric isotropic luminosity and can, at least during flaring states, dominate the luminosity in all other bands by a factor ~ 10 or more. With spectra extending to GeV and TeV energies, variability timescales measuring less than a day, and apparent luminosities reaching 10^{48} – 10^{49} ergs s^{-1} (e.g., Mattox et al. 1997), extremely energetic sites of nonthermal particle acceleration must be involved. (For reviews of gamma-ray blazars and blazar variability, see Hartman et al. 1997 and Ulrich et al. 1997, respectively.)

Almost all of the AGNs that have been detected by EGRET are blazars. The term blazar refers to BL Lac objects as well as to highly variable and strongly polarized quasars. Blandford & Rees (1978) first suggested that blazar properties can be explained by a model involving relativistic plasma outflows ejected from accreting supermassive ($\sim 10^6$ – 10^9 Solar mass) black holes (see also Blandford & Königl 1979; Rees 1984). According to this scenario, strong polarization, rapid variability, and superluminal motion are observed nearly along the jet axes. The existence of such jets is implied by VLA images of extended lobes of radio galaxies (Begelman et al. 1984).

Gamma-ray observations extend and test this model. The more rapidly varying emission at high energies is thought to arise from regions much closer to the central engine than can be directly imaged at other wavelengths. Extremes of photon or magnetic field density must prevail near the black hole engine to drive collimated bulk plasma, Poynting flux, or pair outflows. Multiwavelength analyses, which combine timing and spectral information can be used to determine the location of the acceleration and emission sites in the jet. GLAST observations of the inner regions of jets may revolutionize studies of the jet-disk symbiosis in sources such as 3C 273, where temporal correlation analyses of ultraviolet bump, synchrotron,

and gamma-ray jet emission can reveal conditions leading to flares. Multiwavelength campaigns have proved crucial for understanding AGN in general, and blazars in particular. Good examples are the campaigns for 3C 279 (Maraschi et al. 1993; Wehrle et al. 1998) and Mkn 421 (Macomb et al. 1995; Takahashi et al. 1996; Takahashi et al. 2000). Such campaigns involve many ground-based observatories, sensitive in the radio, infrared, optical, and TeV gamma-ray ($\S 10$) bands, but also take advantage of space-borne platforms, sensitive in the X-ray and soft gamma-ray bands. Fortunately, several current and planned X-ray astronomy missions are expected to be in operation during the GLAST mission, including Chandra, XMM, Integral, and Astro-E II.

3.1 Blazar Models

The broadband νF_ν spectra of blazars generally show two pronounced components: a lower-frequency component peaking between radio and X-ray energies, and a high frequency component peaking in gamma rays (see Fig. 3-1). Because the former is substantially polarized, it is generally thought to be synchrotron emission from energetic nonthermal electrons and positrons accelerated at a shock front. In red blazars, the νF_ν synchrotron component peaks in the infrared. Synchrotron flux peaks at UV and X-ray energies for blue blazars. Of the four blazars that have been detected at TeV energies, three are blue blazars (namely Mrk 501, PKS 2155-304, and 1ES 2344+514) and the fourth, Mrk 421, is somewhere in the middle. The bluer the blazar, the less luminous (Fossati et al. 1998). This may result from differences in outflow Lorentz factors (Kubo et al. 1998). A major unsolved problem is how the galaxies “cool their jets,” that is, how the environment of the host galaxy produces different energy losses on the radiating electrons in their jets. Solving this problem would clarify the processes leading to galaxy formation, particularly formation of the disturbed and elliptical galaxies that are more likely to be jet sources.

Blazars are powerful and highly variable at all frequencies, but their implied isotropic luminosities and the doubling and halving timescales of their emission reach extremes at gamma-ray energies. Compactness analyses show that relativistic beaming with bulk Lorentz factors $\Gamma > 5$ – 10 is required in order to avoid absorption of the gamma rays via $\gamma\text{-}\gamma \rightarrow e^+e^-$ pair

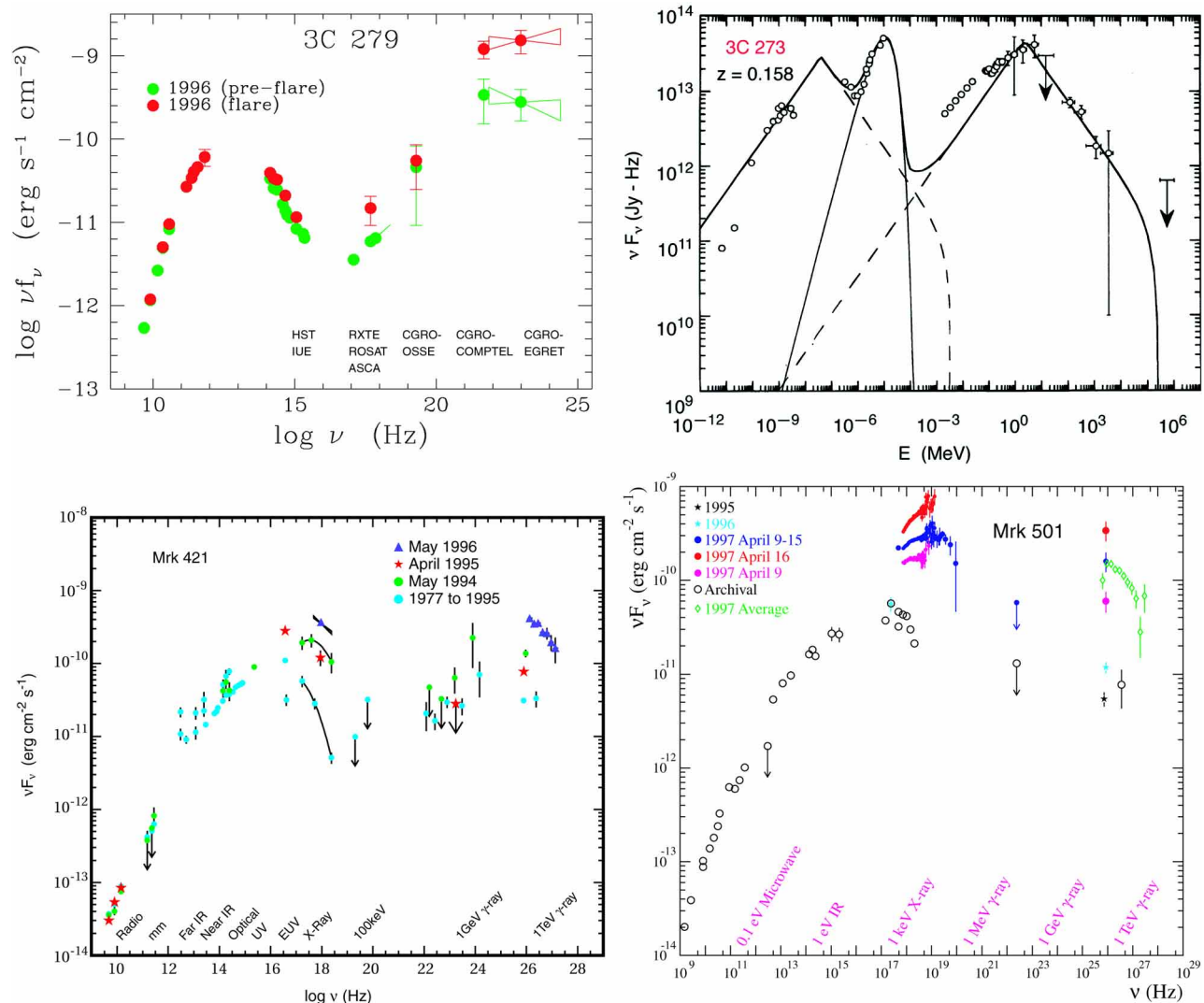


Figure 3-1 Spectral energy distributions of the quasars 3C 279 (top-left) and 3C 273 (top-right), the BL Lac object Mrk 421 (bottom-left), and the blue blazar Mrk 501 (bottom-right) at various epochs. Note the dominance of the gamma-ray flux in 3C 279 during the flaring state. The 3C 273 spectrum displays a model with jet synchrotron, accretion disk, and jet external Compton radiation.

production attenuation (Maraschi et al. 1992; Dermer & Gehrels 1995; Mattox et al. 1997). Gamma-ray observations have yielded new tests for beaming on the basis of correlated emissions of the synchrotron and gamma-ray components (Catanese et al. 1997). Multiwavelength campaigns employing GLAST and new space-based X-ray detectors may reveal values of Γ that are larger than those implied by radio measurements of superluminal motions (e.g., Vermeulen & Cohen 1994). High-quality GLAST observations will permit charting the time dependence of the bulk Lorentz factor of the radiating plasma to distinguish between accelerating and decelerating jet models of blazar AGNs (Marscher 1996).

Sensitive high-energy observations with GLAST will test leptonic and hadronic models of the jets. In

leptonic models of blazars, the main source of gamma rays is Compton scattering of soft photons by energetic nonthermal electrons and positrons in the jet. The source of the soft photons is controversial: synchrotron self-Compton (SSC) models (Maraschi et al. 1992; Marscher & Bloom 1994) employing the leptons' own (self-) synchrotron radiation is one possibility. The external Compton scattering (ECS) scenario is another, where photons from an accretion disk or torus enter the jet directly (Dermer et al. 1992; Protheroe & Biermann 1997) or after being scattered by broad-line region clouds (Sikora et al. 1994; Blandford & Levinson 1995). Most of the ambient photons are likely to be near-infrared emission from hot dust in the disk (Blazewski et al. 2000). Another variant of the ECS model argues that beamed synchrotron photons are

echoed back into the jet after being scattered from gas and dust in the jet's path (Ghisellini & Madau 1996). Coordinated H- α and GLAST gamma-ray observations could test the synchrotron echo scenario (Koratkar et al. 1998). Most likely, the SSC and ECS processes are both present, perhaps with the SSC process dominating in blue blazars or in red blazars near quiescence, and the ECS process dominating when the sources are flaring. Coordinated X-ray and GLAST gamma-ray observations could distinguish between SSC and ECS models (Böttcher 1999).

Gamma rays from blazar jets could also originate from accelerated protons and hadrons (Mannheim & Biermann 1992; Gaisser et al. 1995) that interact with ambient particles through secondary ($pp \rightarrow \pi X$) production, or with ambient photons through photomeson ($p\gamma \rightarrow \pi X$) or photo-pair ($p\gamma \rightarrow e^\pm X$) production. The pairs produced in these processes can initiate an electromagnetic cascade through Compton and synchrotron processes, leading to emergent power-law photon spectra. Sikora & Madejski (2000) find that neither pure leptonic or pure hadronic models alone can explain their X-ray observations of blazar jets. GLAST will for the first time discriminate between leptonic and hadronic models by comparing the decay characteristics of the synchrotron and gamma-ray components during flares (Böttcher & Dermer 1998). Evidence for high-energy protons in blazar jets would spur studies of cosmic-ray acceleration in relativistic shocks and the development of more sensitive neutrino detectors to search for evidence of neutrinos from AGNs.

3.2 AGN Observations with GLAST

GLAST will probe the physics of relativistic jets by providing energy- and time-resolved spectra of blazars in quiescence and during flares. Weak evidence from PKS 0528+134 suggests that blazar spectra during flares are harder than in quiescence (Mukherjee et al. 1997). GLAST will determine whether this is a general property of blazars, and analyses will show if this indicates an effect of radiative cooling or bulk plasma deceleration. If spectra harden with time, then this might indicate that the jet plasma is energized by sweeping up ambient material.

Fig. 3-2 compares the EGRET observations of PKS 1622-297 and 3C 279 with simulated GLAST measurements based on models that are consistent with the EGRET data. GLAST observations of finer temporal structure in flaring light curves will improve limits on the Doppler factor through compactness

arguments and on the sizes of the event horizons of the central black holes. Models for the energization of the jet will be tested by measuring spectral index evolution, as shown in Fig. 3-2, where a spectral index/hardness correlation in the 3C 279 flare light curve is assumed.

GLAST may discover a new class of high-energy gamma-ray sources associated with radio galaxies. An EGRET source is coincident with the location of Centaurus A (Sreekumar et al. 1999), the brightest AGN in the hard X-ray sky and one of the nearest. If Cen A is the source of the gamma rays, then it is the only AGN detected by EGRET that does not display strong blazar properties. However, evidence from OIII emission maps suggests that Cen A is a misaligned blazar (Morganti et al. 1992). As shown in Fig. 3-3, GLAST could confirm the EGRET detection and potentially discriminate between central nuclear emission and a source on the periphery of Cen A if the gamma rays originated from, for example, a microquasar (a much less massive jet-emitting compact object that is not associated with the central black hole in the galaxy). A GLAST discovery that radio galaxies are high-energy gamma-ray sources would provide valuable information about the parent population of blazars and the energy dependence of the beaming cones of blazars. Once the beaming cone is known, statistical studies can establish the paternity of BL Lacs and quasars to FR1 and FR2 galaxies (Urry and Padovani 1995).

Despite the soft gamma-ray detections of many Seyfert galaxies (see Johnson et al. 1997 for review), none has been detected with EGRET. Seyfert nuclei may lack highly relativistic particles, since the high-energy Seyfert spectra are successfully interpreted in the context of processes occurring in the accretion disk. Most current models rely on thermal Comptonization of optical/UV photons emitted by the accretion disk by transrelativistic thermal plasma. A detection of MeV/GeV gamma-ray emission – or even the very sensitive limits GLAST could provide for the non-blazar class of AGNs – would provide insights about the release of gravitational energy during accretion.

3.3 Blazar Cosmology with GLAST

EGRET detected more than 70 blazar AGNs with redshifts ranging from 0.03 to 2.3, and a mean redshift near $z = 1$. GLAST will detect several thousand such objects (Figs. 3-4 and 3-5), possibly back to the time of their formation. This will permit the construction of luminosity functions for the various subclasses of blazar AGNs and a study of their evolution with cosmic time,

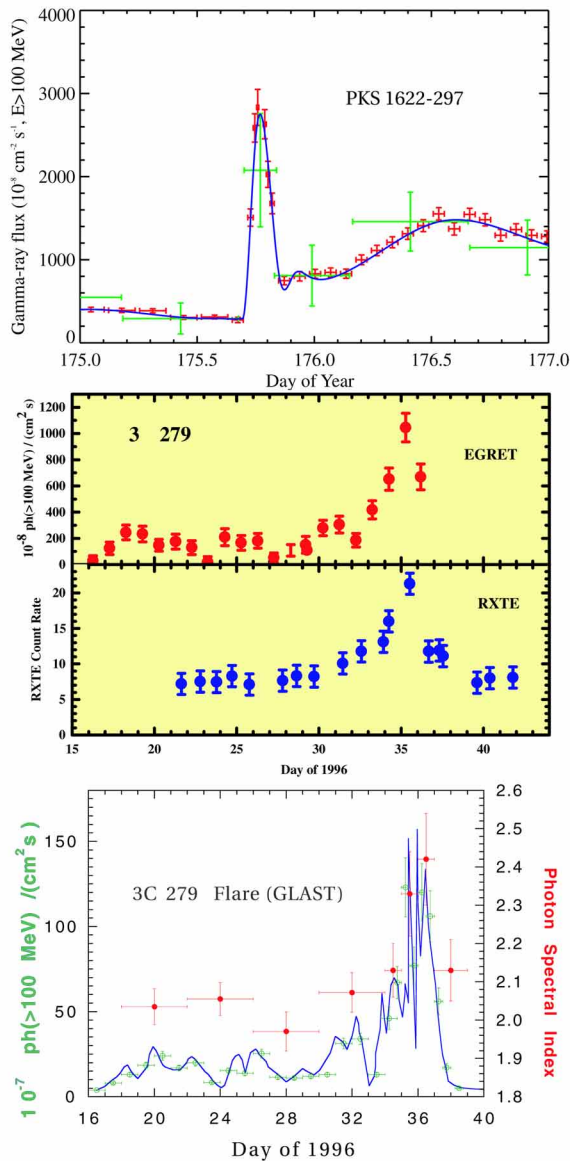


Figure 3-2 (top) EGRET light curve (green points) for two days during the 1995 flare of blazar PKS 1622-297 (Mattox et al. 1997) together with a simulated GLAST light curve (red points). The solid line is a plausible hypothesis for the actual flux. The error bars are $1-\sigma$. The GLAST light curve is calculated under the assumption of inertial pointing at PKS 1622-297 and includes the effects of occultation by Earth. (middle) Flare observed from 3C 279 in 1996 with EGRET and RXTE (Wehrle et al. 1998). (bottom) Simulated GLAST observations of spectral index evolution of 3C 279 for a light curve consistent with the EGRET flare.

which can be compared with the evolution of radio quasars and the star formation history of the universe (see Chiang & Mukherjee 1998). Among the important questions to be addressed by GLAST are whether all blazars emit high-energy gamma radiation, what the

duty cycles of these emitters are, and whether the combined emission of the fainter blazars is sufficient to make up the “isotropic” high-energy gamma radiation that SAS-2 and EGRET have observed. As the gamma-ray background is resolved into discrete sources, the fraction that could be due to the annihilation or decay of exotic particles (see §5) decreases.

By observing blazars at various redshifts between the EGRET energy range (~ 30 MeV–10 GeV) and that now observed by ground-based Cherenkov telescopes (above ~ 300 GeV), GLAST will explore the important energy range where the spectra of most blazars are expected to cut off. These cutoffs could be due either to intrinsic absorption (Stecker et al. 1996) or to interactions of blazar gamma rays with photons of the extragalactic infrared-UV background light (EBL; Stecker et al. 1992). If the high-energy spectral cutoffs are primarily caused by interactions with EBL photons (which can be established by regular monitoring of blazar spectra and variability to deduce an underlying nonvarying absorber), the cutoff energy should vary inversely with redshift in a predictable way (Salamon

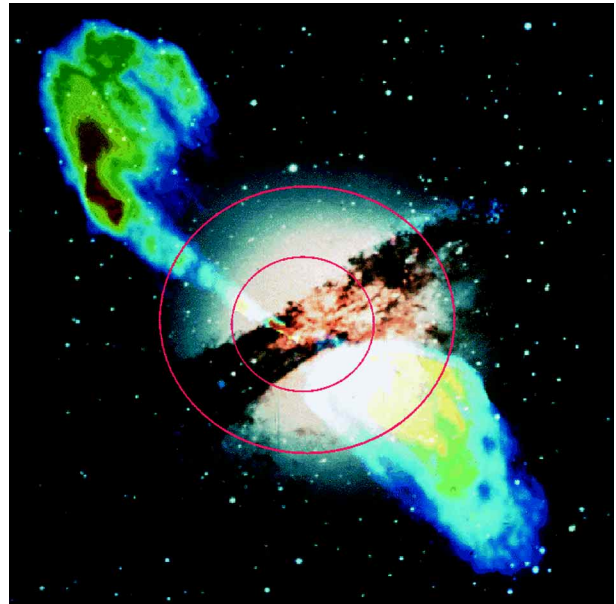


Figure 3-3 Montage of optical and radio continuum images of Centaurus A with simulated 68% and 95% confidence level contours representing GLAST’s localization capability during a 1-year sky survey. The mean flux of Cen A is assumed to be 1.4×10^{-7} $\text{cm}^{-2} \text{s}^{-1}$ (>100 MeV), equal to the flux of the coincident EGRET source 3EG J1324-4314 (Hartman et al. 1999). The angular extent of the radio lobes shown (the ‘inner’ lobes of Cen A) is $\sim 11'$. The EGRET 68% error contour is a few times larger than the entire figure.

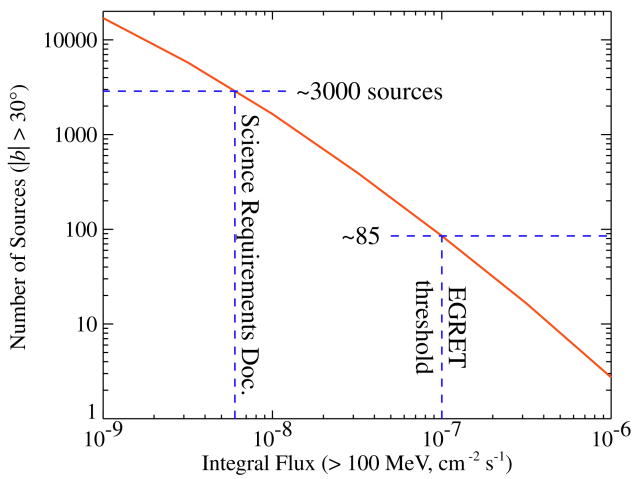
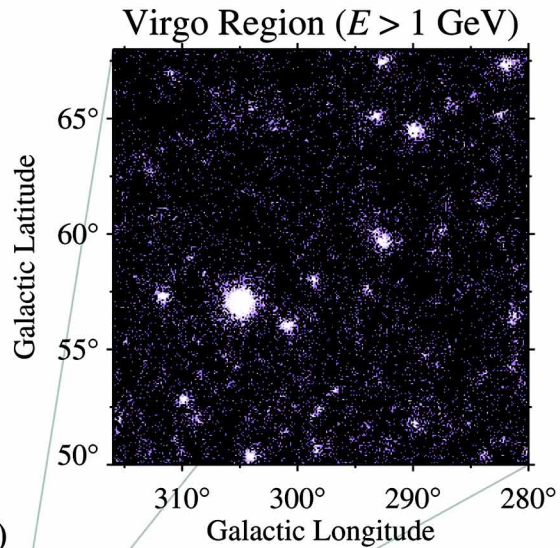


Figure 3-4 Estimate of the number of AGNs that GLAST will detect at high latitude in a 1-year sky survey compared to EGRET's approximate detection limit. The gamma-ray $\log N$ - $\log S$ relation for AGNs is from Stecker & Salamon (1996). Note that the range $|b| > 30^\circ$ spans *half* the sky.

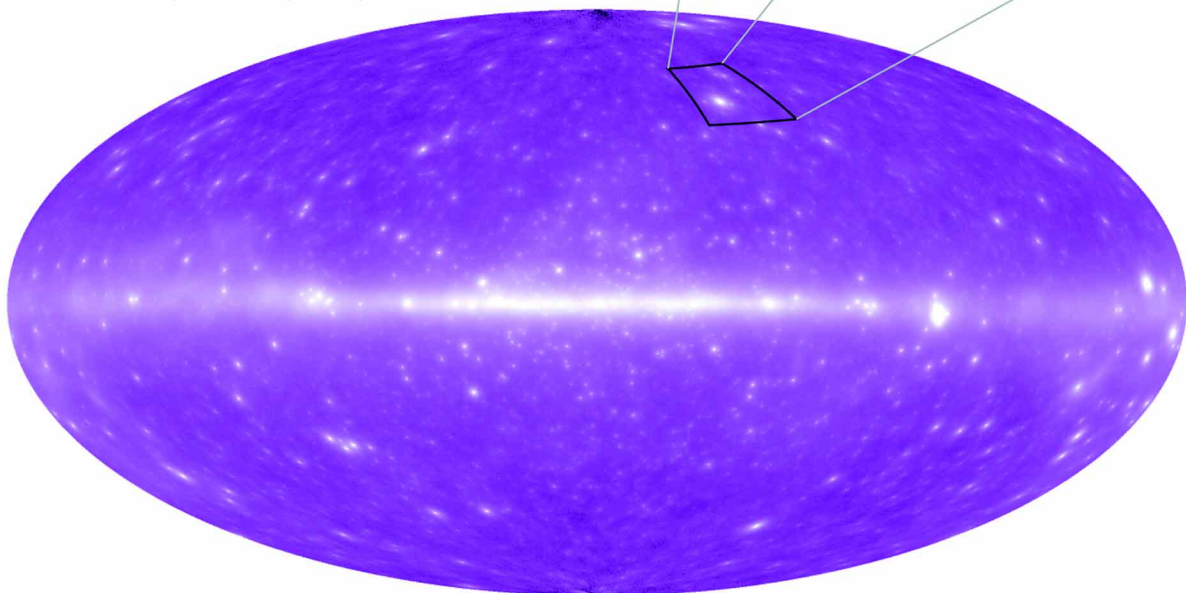
Figure 3-5 Simulated intensity map for a 1-year sky survey with GLAST. The map is in Galactic coordinates, and the bright band across the center is diffuse emission from the Milky Way. The point sources at intermediate and high latitudes are simulated AGNs matching the $\log N$ - $\log S$ relation of Stecker & Salamon (1996), and having integrated intensity equal to the unresolved isotropic intensity observed by EGRET (Sreekumar et al. 1998). The inset is the simulated distribution of photons in the Virgo region for energy greater than 1 GeV.

& Stecker 1998). If such is the case, GLAST spectra of blazars at various redshifts will be an important probe of the EBL, and therefore of star-forming activity, as a function of redshift.

The EBL is an integral measure of starlight emitted and reprocessed during galaxy formation. A complete calculation requires a population synthesis model of galaxies which treats gravitational collapse and merging of dark matter halos, gas cooling and dissipation, star formation, supernova feedback and metal production (MacMinn & Primack 1996; Primack et al. 1999). High-energy gamma-ray absorption of distant blazars may be used to test assumptions about the stellar initial mass function and the underlying cosmology. GLAST measurements of absorption of blazar spectra as a function of redshift could provide an independent probe of the star formation history of the universe.



GLAST Sky Survey (1-year, $E > 100$ MeV)



4. Unidentified Sources

More than 60% of the known high-energy gamma-ray sources are unidentified. In the Third EGRET Catalog, shown in Figure 4-1, 170 of the 271 sources have no established counterparts at other wavelengths (Hartman et al. 1999).

Commonly held (and incorrect) beliefs about gamma-ray bursts (§6) before the Compton Observatory may provide a useful analogy to the unidentified EGRET sources. Before CGRO, there was a near consensus that the gamma-ray bursts were powerful, but not spectacular, flashes associated with nearby neutron stars. It was expected that the Burst and Transient Source Experiment (BATSE) on CGRO would verify these predictions. The results are well known: BATSE observed an isotropic distribution of sources, implying that bursts originate at cosmological distances and emit prodigious amounts of energy (Meegan et al. 1992). Clearly, an unknown class of objects has the potential for the most remarkable discoveries.

What is known about the unidentified EGRET sources is quite limited:

- Each must be a powerful, nonthermal particle accelerator.

- The lack of obvious counterparts implies high values of L_γ/L_{X-ray} , L_γ/L_{opt} , and L_γ/L_{radio} .
- Many sources clustered along the Galactic plane appear to be correlated with star-forming regions or supernova remnants (Yadigaroglu & Romani 1997; Romero et al. 1999).
- Some are time variable, while others have steady emission (McLaughlin et al. 1996; Tompkins 1999). The variable sources seem to include both Galactic and extragalactic populations.
- The high-latitude sources have an isotropic component and one likely to be a local Galactic population (Ozel & Thompson 1996; Grenier 1999).
- Steady, medium latitude sources may be associated with Gould's Belt, the massive star-forming regions arrayed on an expanding shell of gas that surrounds the solar neighborhood (Gehrels et al. 2000).

4.1 GLAST Observations of Unidentified Sources

GLAST will be the breakthrough instrument for unraveling the mysteries of the unidentified sources. For the first time, a gamma-ray telescope will have the

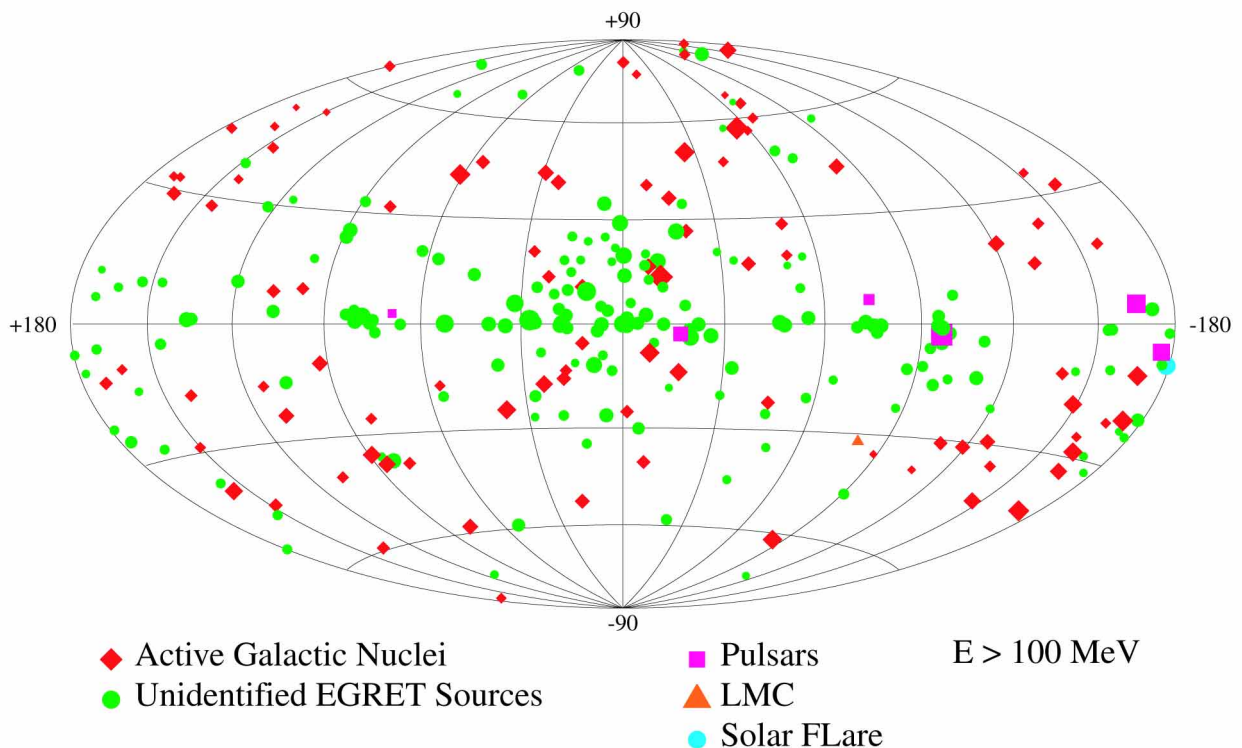


Figure 4-1 Third EGRET Catalog of high-energy gamma-ray sources (Hartman et al. 1999). The source locations are shown in Galactic coordinates.

combination of sensitivity and angular resolution to tie the gamma-ray sources to specific objects (Fig. 4-2). How GLAST will accomplish this goal will depend on what the sources turn out to be. Here are some of the possibilities:

- *Previously-unknown blazar-class AGNs.* The source 3EG J0433+2908, for example, was identified with a radio/optical/infrared source that has the characteristics of a BL Lac object, following the detection of a gamma-ray flare during a high state of the radio emission (Lundgren et al. 1995). The wide field of view and high sensitivity of GLAST will readily catch such flares; the arc-minute-scale error boxes will then allow comparison with a manageable number of radio and optical sources to search for correlated flaring activity.

- *Previously unknown pulsars.* It would be remarkable if Geminga were the only radio-quiet pulsar, and indeed models predict that more pulsars should be visible in gamma rays without strong radio emission (Yadigaroglu & Romani 1995). Mirabal & Halpern (2001) recently concluded that the bright, steady unidentified source 3EG J1835+5918 is a radio-quiet pulsar associated with a faint X-ray source RX J1836.2+5925 (Fig. 4-3). GLAST will have sufficient sensitivity and resolution for direct pulsation searches in the gamma-ray data, independent of observations at other wavelengths (see §7). Harding & Zhang (2000) propose that the steady sources in the Gould Belt (Grenier 1999; Gehrels et al. 2000) may be gamma-ray pulsars observed outside of their radio beams. They find that the faint fluxes and steep spectra of these sources are well-matched by this model.

- *Binary Systems.* 3EG J0241+6103 (2CG 135+01) is consistent in position with the variable radio source GT0236+610, also seen at optical and X-ray energies and thought to be a binary system. Particles may be accelerated by shocks at the boundaries between strong winds from the two companions (Tavani et al. 1998). EGRET may have seen evidence for GeV gamma-ray emission from the X-ray binary Centaurus X-3 (Vestrand et al. 1997). Accurate positioning of the sources and spectral measurements are critical to confirming these identifications. All such sources are time variable, and GLAST will be well suited to monitoring them with its wide field of view.

4.2 Potential New Source Classes

Several potential new classes of sources have been proposed to explain unidentified Galactic and extragalactic sources. In some cases, the proposed classes are presently represented by only one EGRET

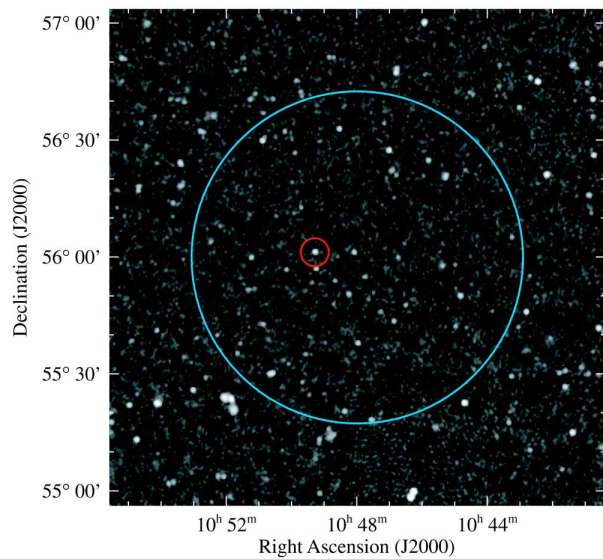


Figure 4-2 Relative sizes of EGRET (blue) and GLAST (red) 95% confidence contours shown on a portion of the 1.4 GHz NRAO VLA Sky Survey (Condon et al. 1996). The EGRET error circle shown has the average area for sources in the Third EGRET Catalog (Hartman et al. 1999). The GLAST error circle is for a moderately strong source below the detection threshold for EGRET.

source. GLAST will be able to sort out the candidates and study the physics of any new classes.

The variable source 3EG 1809-2328, which is probably Galactic, may be due to pulsar winds interacting with a neighboring molecular cloud (Oka et al. 1999). The persistent source 3EG J1746-2851, associated with the Galactic center, is also a mystery (Mayer-Hasselwander et al. 1998). Among the suggestions for the origin of this source is advection onto the black hole at the center of the Galaxy.

A different type of EGRET source, 3EG J1837-0423, was detected as a transient, flaring for only a few days: this is reminiscent of a blazar and very unlike the pulsars, which are always visible. However, the error box for this source contains no radio source at a flux level consistent with blazars seen by EGRET. This is probably the best candidate for an astrophysical accelerator of a new type (Tavani et al. 1997).

Paredes et al. (2000) report the discovery of the Galactic microquasar LS 5039 and note that it is coincident with the unidentified EGRET source 3EG J1824-1514. Microquasars are X-ray binary systems that exhibit many of the properties of active galaxies, including the emission of superluminal jets.

Totani & Kitayama (2001) propose that

unidentified, steady, high-latitude gamma-ray sources may be clusters of galaxies in the process of forming. The gamma-ray emission would originate from interactions between intracluster gas and high-energy electrons, that are accelerated by shocks in the gas.

Other suggestions for high-energy gamma-ray sources include accreting isolated black holes (Dermer 1997), Kerr-Newman black holes (Punsley 1998), Wolf-Rayet stars (Kaul & Mitra 1997), and ‘hot spots’

left as artifacts of Galactic gamma-ray bursts (Plaga et al. 1999). GLAST’s ability to detect more sources, measure positions more accurately, determine energy spectra over a broad range, and track time variability on many scales will all help to correlate the gamma-ray detections with sources found in the deep observations in other wavebands. The timescales and spectral evolution of the variations in flux also can be used to discriminate between source models.

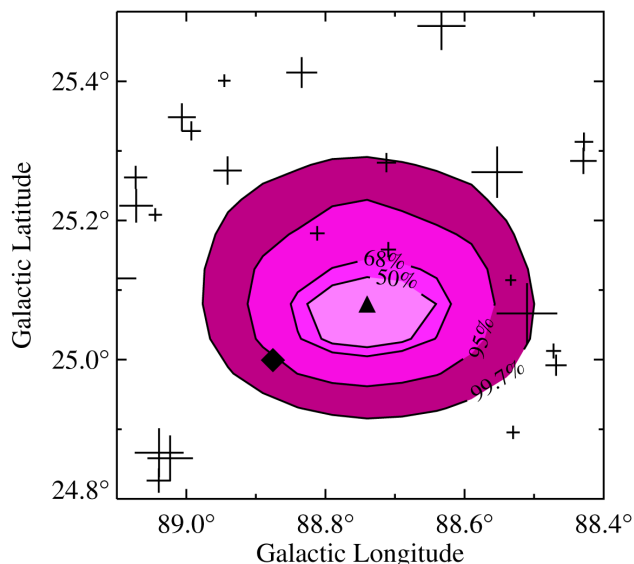


Figure 4-3 EGRET source location map for 3EG J1835+5918 (Hartman et al. 1999), an intense, apparently steady source with no X-ray or radio counterpart. The crosses are positions of radio continuum sources in the 1.4 GHz NRAO VLA Sky Survey (Condon et al. 1996). The sizes of the crosses are related to the fluxes; the faintest are only ~ 10 mJy. The diamond indicates the location of the X-ray source RX J1836.2+5925 proposed to be the neutron star responsible for the gamma-ray emission (Mirabal & Halpern 2001).

5. Cosmology and the Diffuse Background

An apparently isotropic, presumably extragalactic, component of the diffuse gamma-ray flux was discovered by the SAS-2 satellite and confirmed with EGRET (Thompson & Fichtel 1982; Sreekumar et al. 1998) for energies in the range above 30 MeV. What is responsible for this flux of gamma rays? There are a number of possibilities. The most prosaic, and thus perhaps the most likely, is composite light from a large number of faint point sources, such as AGNs (Stecker & Salamon 1996; §3). Another, more exotic possibility which would imply exciting particle-astrophysics is relic radiation from some yet-unknown high-energy process in the early universe, such as neutralino decay in R-parity violating versions of supersymmetric extensions of the standard model of particle physics (SUSY).

Through the era subsequent to COS-B, when 3C 273 was the only extragalactic point source detected, the composite AGN-light hypothesis could not be tested. More point sources had to be characterized so that an extrapolation of their intensity and energy distributions could be attempted. Study of the isotropic

flux was greatly advanced with EGRET, due to its lower instrumental background and greater sensitivity. Dozens of extragalactic sources have been detected (von Montigny et al. 1995; Hartman et al. 1999), and many have been identified with the blazar class of AGNs (§3). Sreekumar et al. (1998) analyzed the uniformity and spectrum of the isotropic flux observed by EGRET. Removal of the contributions from resolved point sources was challenging, owing to the large size of the EGRET point-spread function. The foreground Galactic flux, mostly originating from cosmic-ray interactions with interstellar nuclei and photons (§8), also had to be subtracted carefully. The results indicate that the energy spectrum of the isotropic emission is well described by a power law with photon spectral index $\alpha = 2.1 \pm 0.3$ over EGRET’s energy range. The emission appears to be isotropic on the $\sim 30^\circ$ angular scales of the study, although the systematic uncertainties remain fairly large. The spectral index is consistent with the average index for blazars that EGRET detected, which lends some support to the hypothesis that the isotropic flux is from unresolved

blazars. The actual source fraction is difficult to infer, but has recently been estimated to be $\sim 75\%$ (Chiang & Mukherjee 1998) and 40–80% (Mücke & Pohl 2000). These findings depends sensitively on poorly known parts of the gamma-ray luminosity function for blazars (Chiang et al. 1995).

5.1 Deep Survey of Diffuse Background for Signatures of Unstable Particle Relics

GLAST will vastly increase the number of detected point sources, with a flux limit at high latitudes that is a factor of 30 or more lower than EGRET's (Table 1-1). Whereas EGRET identified about 70 AGNs, GLAST should see thousands, as discussed in §3, and thus resolve a greater fraction of the isotropic emission. GLAST will have much more uniform exposure at high latitudes, and because its sensitivity will not vary with time (unlike EGRET), the large scale isotropy of the diffuse emission will be much better determined (Willis 1996). Any truly diffuse component that remains would be of great interest, and would rank as one of the most important discoveries of GLAST.

Truly diffuse extragalactic gamma-ray emission could originate in decays of exotic particles in the early universe. The energy spectrum of this component should be different from the AGN contributions. Figure 5-1 shows that the large effective area of GLAST, especially at high energies, may permit a statistically significant detection of this spectral difference (Kamionkowski 1995; Willis 1996). Recently, bounds on long-lived relics have been derived using EGRET

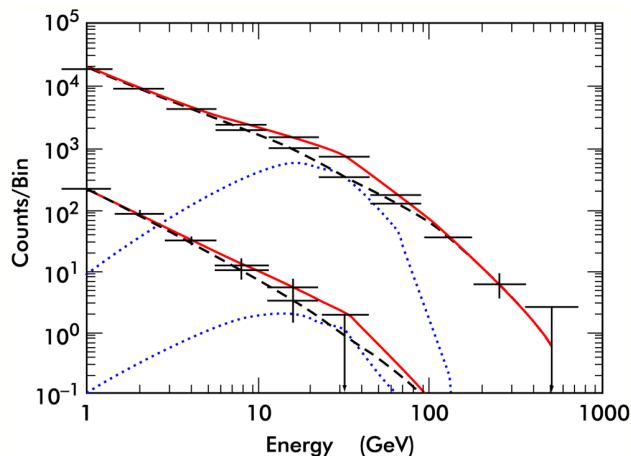


Figure 5-1 Simulated diffuse extragalactic gamma-ray flux measurements for GLAST (upper points) and EGRET (lower points). The dashed lines show the flux from unresolved AGNs, the dotted lines the contributions from WIMP decays in the early universe, and the solid line shows the total (Willis 1996).

and COMPTEL observations of the diffuse gamma-ray background (Kribs & Rothstein 1997). Many models predict long-lived relics that may or may not be dark matter candidates. Long lifetimes for heavy relics, where “long” means within several orders of magnitude of the age of the universe, may arise in models which have symmetries that are broken only at short distances. Examples of such models are technibaryons in technicolor models or the lightest supersymmetric particle in an R-parity violating SUSY model.

Figure 5-2 shows the dominant scattering mechanisms for high-energy photons injected in the post-recombination era of the universe. The universe is essentially transparent to $z \sim 700$ for $100 \text{ MeV} < E_\gamma < 100 \text{ GeV}$ (at the source), neglecting scattering from the EBL (see §3). Note that emission of a gamma ray of $E_\gamma < 300 \text{ GeV}$ at $z > 100$ corresponds to $E_\gamma < 15 \text{ GeV}$ at $z \sim 5$, the beginning of the era of galaxy formation. This implies that the EBL will negligibly absorb such photons.

From EGRET and COMPTEL measurements of the extragalactic diffuse background, Kribs & Rothstein (1997) estimated final density bounds for a relic particle that has three-body radiative decays. On the assumption that the relic has roughly the critical density, their analysis shows that relic lifetimes, τ_χ , in the range $3 \times 10^4 \text{ years} < \tau_\chi < (3 \times 10^{21} - 3 \times 10^{23}) \text{ years}$, for relic masses $M_\chi = 50 \text{ GeV} - 10 \text{ TeV}$, are excluded (compare

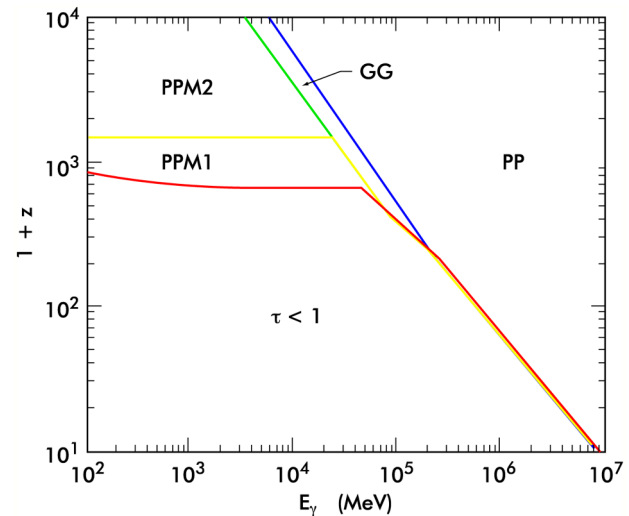


Figure 5-2 Dominant scattering mechanisms for high-energy photons injected in the post-recombination era. The region below the red line has an optical depth $\tau < 1$, thus no scattering occurs. The other regions are dominated by e^+e^- pair production (PP), photon-photon scattering (GG), pair production in matter (PPM1) and pair production in ionized matter (PPM2) (Kribs & Rothstein 1997).

to proton lifetime limits of $>10^{33}$ years). In addition, relics with densities considerably below the critical density are excluded, which places a strong constraint on models with a long-lived massive particle. GLAST measurements should extend the mass, lifetime, and relic density limits by at least two orders of magnitude. This improvement is expected due to the much larger energy range and sensitivity of GLAST as compared to EGRET, as well as the ability of GLAST to resolve contributions of point sources to the extragalactic background.

5.2 Gamma-Ray Lines from Supersymmetric Particle Dark Matter Annihilation

The dark matter puzzle is one of the central challenges confronting particle astrophysics and cosmology. The measured rotation curves of galaxies, the confinement of intergalactic gas by galaxy clusters, and large-scale structure formation arguments are powerful evidence for dark matter. Evidence for dark matter in galaxies and the universe is reviewed in Ashman (1992) and Trimble (1989), respectively. (Also see Kamionkowski & Spergel 1994 for recent arguments based on structure formation.) The lightest supersymmetric particle (LSP), χ , is a reasonable, and perhaps the most promising, candidate for the dark matter of the universe (Weinberg 1983; Goldberg 1983). It is neutral (hence the name neutralino), and stable if R parity is not violated. Supersymmetry seems to be a necessity in superstring theory (and M-theory) which potentially unites all the fundamental forces of nature, including gravity. If the scale of supersymmetry breaking is related to that of electroweak breaking, then this density Ω_χ may be the right order of magnitude to explain the nonbaryonic dark matter. Although the highest-energy accelerators have begun to probe regions of SUSY parameter space, the limits set at this time are not very restrictive. With the requirement that neutralinos make up most of the dark matter, current limits allow viable models in the mass interval, $30 \text{ GeV} < M_\chi < 10 \text{ TeV}$. (For an extensive review of the dark matter candidates and the experimental situation see Jungman et al. 1996.) If neutralinos make up the dark matter of the Milky Way, they have nonrelativistic velocities. Hence, the neutralino annihilation into the $\gamma\gamma$ and γZ final states would give rise to gamma rays with unique energies, that is, gamma-ray lines with $E_\gamma = M_\chi$ or $E_\gamma = M_\chi(1 - m_Z^2/4M_\chi^2)$. The neutralino signal in its various guises has been thoroughly discussed in the literature (Jungman, Kamionkowski & Griest 1996 and references therein,

and more recently, Bergström, Ullio & Buckley 1998; BUB). GLAST can search for gamma-ray lines in the mass range above 30 GeV with significant sensitivity when compared to other types of searches if the energy resolution goal for the LAT, $\sigma_E/E \sim 3\text{--}4\%$ (§1), is achieved.

Recently, full one-loop calculations of the $\chi\chi \rightarrow \gamma\gamma$ (Bergström & Ullio 1997; Bern et al. 1997) and $\chi\chi \rightarrow \gamma Z$ (Ullio & Bergström 1998) annihilation processes have been performed for the first time in the minimal supersymmetric extension of the standard model (MSSM). Compared to older estimates, the newly computed rates are up to an order of magnitude larger.

Different models have been proposed for the distribution of the nonbaryonic dark matter in the Milky Way. Recent N-body simulations of dark matter halos have, however, given indications of a universal profile where the density increases substantially near the galactic center (Navarro, Frenk & White 1996; NFW). This model, which enhances the $\chi\chi$ annihilation rate compared to past models of halo distributions of dark matter, was used for the $\chi\chi$ annihilation calculations of BUB. They found that the gamma-ray line emission from the halo should be detectable in the GLAST sky survey for some ranges of MSSM parameter space. Their limits indicate that GLAST will explore a significantly larger portion of the MSSM phase space than other types of searches, in the range $50 \text{ GeV} < M_\chi < 200 \text{ GeV}$, particularly for the higgsino-like neutralino for the $\chi\chi \rightarrow \gamma\gamma$ case.

If $\chi\chi$ annihilations in the halo do produce a monochromatic gamma-ray signal, then in most cases an even larger continuum diffuse component due to annihilations into quark jets should also be present, and may also be detectable by GLAST.

6. Gamma-Ray Bursts

Gamma-ray bursts (GRBs) are the most intense and most distant known sources of high-energy gamma rays; at GeV energies, the brightest GRBs are 1000-10,000 times brighter than the brightest AGN. The unparalleled luminosities and cosmic distances of GRBs, combined with their extremely fast temporal variability – full amplitude variations in milliseconds – make GRBs an extremely powerful tool for probing fundamental physical processes and cosmic history.

The LAT in concert with the GBM will measure the energy spectra of GRBs from a few keV to hundreds of GeV during the short time after onset when the vast majority of the energy is released. GLAST will also promptly alert other observers, thus allowing the observations of GLAST to be placed in the context of multiwavelength afterglow observations, which are the focus of HETE-2 and the upcoming Swift missions. The additional information available from GLAST's spectral variability observations will be key to understanding the central engine as can be seen, for example, in the theoretical predictions of Figure 6-1.

After more than thirty years of study at gamma ray energies, and the detection of more than 3,000 bursts (see Fishman and Meegan, 1995) afterglows from GRBs were discovered at X-ray energies (Costa et al. 1997). Convincingly predicted by fireball models describing the extremely relativistic expanding ejecta (Meszaros and Rees, 1997), afterglows have now also been observed at optical, infrared and radio wavelengths demonstrating that some GRB sources lie at cosmological distances (e.g. Metzgar et al.) with redshifts ranging up to 5 (e.g., van Paradijs et al. 2000).

Along with mounting evidence that GRBs are associated with star forming regions in distant galaxies, the enormous implied luminosities – up to 10^{54} ergs if isotropic – can make them valuable probes of the very high redshift Universe (Lamb & Reichart 2000) reaching beyond the redshift regime of the most distant quasars.

The inferred range of GRB luminosity is of order ~ 100 , with values up to 10^{54} ergs (if isotropic). The total energy released is over 100 times that from a supernova (inferred from radio observations, and essentially independent of beaming considerations). Popular models for the immensely energetic central GRB engines, hypernovae (Paczynski 1998), collapsars, and mergers of neutron/black hole binary systems are based on a black hole accretion disk scenario and the endpoints of the stellar evolution of massive stars (e.g. Fryer et al. 1999). Because no afterglows have been detected from short duration bursts, and because the gamma-ray spectra of the short bursts differ from the longer ones, there may be more than one type of source.

No matter what the source, a relativistic fireball of electrons and protons must be produced. Protons must be present to transport energy, but the fraction must be small because quasi-thermal emergent spectra are not observed. A common feature of physical models (Piran 1999) is the creation of a rapidly spinning black hole, which provides a preferred axis for beaming along a jet.

The high-energy pulses in GRBs are known to be narrower and to peak earlier than at lower energies;

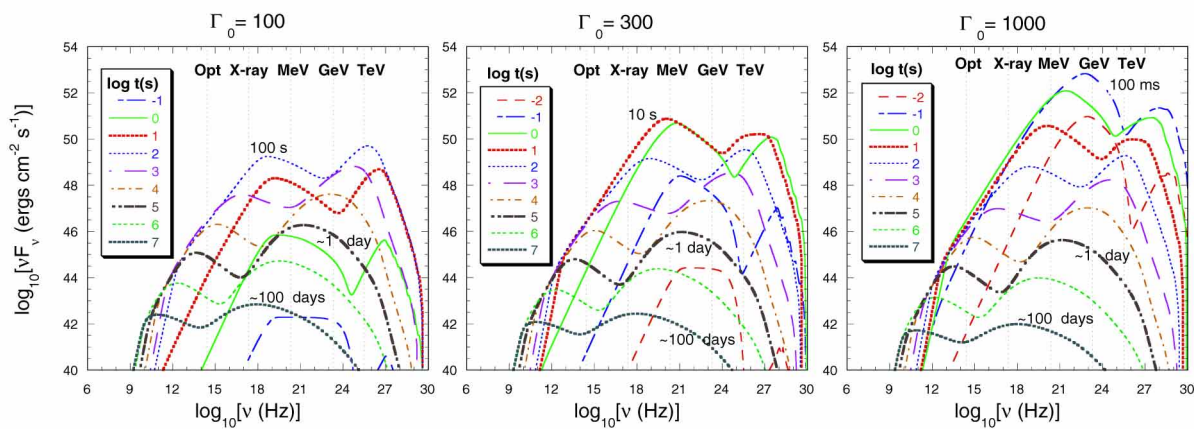


Figure 6-1 The spectral evolution of a GRB produced by the shock created when a blast wave of different initial bulk Lorentz factors Γ interacts with an external medium (Dermer & Chiang 1999). As in active galactic nuclei, two peaks are expected with the lower energy due to synchrotron emission and the higher energy due to inverse Compton scattering.

thus the energy injection mechanism involves short timescales which must be probed at gamma-ray energies. However, the high-energy spectral evolution is very imprecisely mapped at EGRET energies, owing to EGRET's long deadtime, which at ~ 100 ms is comparable to or greater than pulse widths at these energies, and to EGRET's relatively small effective area, which decreased above 500 MeV owing to self-veto in the monolithic anticoincidence shield.

6.1 High-Energy Emission and GRB Models

Prior to the launch of GLAST, missions such as HETE-2 and Swift will provide precise localizations and much will be learned about afterglow properties and the redshift distribution of sources. However, the role of internal shocks in the production of gamma rays and the transition to the fireball/afterglow stage will be revealed only by study at higher gamma-ray energies. The high-energy photons are the (theoretically) most difficult to produce, and are easily lost due to conversion into e^+e^- pairs. Their existence constrains GRB physics in several ways, as described below.

The minimum bulk Lorentz factor of material ejected by a GRB is constrained by the flux of the highest energy gamma rays that escape the source, having survived interaction with keV photons which would produce e^+e^- pairs (Baring & Harding 1997). Only those GeV gamma rays emitted nearly parallel to the more plentiful keV X-rays, as is the case for emission from a relativistically moving source, can escape. The bulk Lorentz factor inferred from high-energy gamma rays also depends on the size of the emission region, which may be inferred from the variability timescale, the observed spectrum (Fig. 6-2), and the distance. EGRET observations suggest Lorentz factors up to a few hundred.

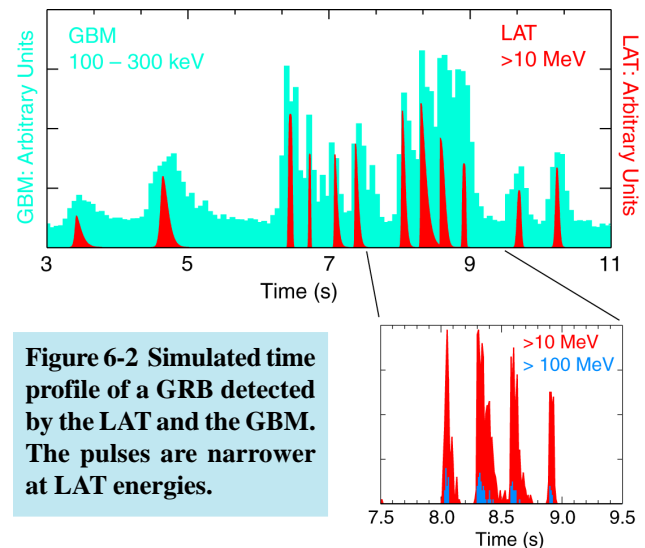
The burst fireball carries both electrons and protons. Very short duration GeV emission is predicted by Dermer et al. (1999) to be the signature of fireballs with the smallest baryon loading: "clean" fireballs have a small baryonic fraction, while "dirty" fireballs have the largest fraction of baryons. Clean fireballs decelerate more rapidly, producing higher-energy gamma rays while the bulk Lorentz factor is still high.

GLAST will be able to investigate the population statistics of the shorter duration, higher energy bursts, constraining the range of electron and proton concentrations in GRB fireballs via inferences of bulk Lorentz factors in sources. The actual conversion of electron and proton energy into gamma rays can occur via several processes, e.g., directly via synchrotron

emission from the particles, or via inverse-Compton interactions with lower energy photons. Observations of the evolution of spectral energy distributions over the full range of a few keV to super-GeV energies will help distinguish the possible mechanisms.

The short deadtime of the LAT will enable the first studies of GRB temporal properties at high energies. Analogous studies using existing data are not possible because at high energies pulse widths are shorter than the 100 ms deadtime of the EGRET instrument. At BATSE energies, the spectral evolution and energy dependence of GRB pulses and pulse structures has already been demonstrated to be crucial in exploring internal versus external shock gamma-ray emission models (Fenimore et al. 1999; Ramirez-Ruiz & Fenimore 1999). Energy dependent lags in pulse structures (Norris et al. 2000) and variability time scales (Fenimore & Ramirez-Ruiz 2000) have also been correlated with GRB luminosities for a limited sample of bursts with known redshifts. Norris et al. find that the lag between hard and soft emission is inversely related to luminosity. A kinematic interpretation of this potentially powerful temporal signature has been explored by Salmonson (2000) based on a variation of Lorentz factor across a relativistic jet. Energy dependent lags and the physics behind GRB temporal properties will be much better studied by the broad energy coverage provided by the combination of the LAT and GBM. Figure 6-2 presents a simulated gamma-ray burst time history, extrapolated from BATSE energies, as viewed by the LAT and GBM. The widths of the pulses decrease significantly with energy (e.g. Ramirez-Ruiz & Fenimore 2000).

Shocks are an efficient method for accelerating particles to high energies. The gamma-ray emission is probably due to internal shocks – faster moving shells



overtaking slower ones, which can easily produce the irregular light curves for which GRBs are famous. External shocks are the probable mechanism for afterglow emission at longer wavelengths. The relativistically expanding fireball will interact with the external medium, gradually sweeping up material; inhomogeneities could produce variable gamma-ray emission. Measurements of spectral evolution at GLAST energies will test this understanding of the roles of internal and external shocks.

The high-energy emission may evolve from a spectrum initially created by electrons interacting via internal shocks, to one dominated by protons interacting with a shock created by the external medium. This temporal evolution of the gamma-ray spectral energy distribution can be correlated with X-ray, optical, and radio afterglows to study the external medium and magnetic fields. Decay of the gamma-ray afterglow should be different from optical and X-ray afterglows. Alternatively, as suggested by Plaga (1995), the gamma-ray afterglow could arise from TeV gamma rays interacting with intergalactic infrared and microwave background radiation to produce e^+e^- pairs, which are deflected by intergalactic magnetic fields (giving rise to the delay), eventually inverse-Compton scattering to produce GeV gamma-rays. If this explanation is correct, it would afford a unique probe of intergalactic magnetic fields.

In one noteworthy burst, GRB 940217, EGRET detected high-energy emission persisting for ~ 5000 s beyond burst cessation at hard X-ray energies (Hurley et al. 1994); this high-energy gamma-ray afterglow contained a significant fraction of the total burst fluence. A few other bright GRBs observed by EGRET also show indications of longer duration emission (Dingus et al. 1997). GLAST will have the sensitivity to detect such afterglows from weaker bursts and for longer durations.

In summary, the highest energy emission in GRBs bears directly on several issues related to the GRB emission mechanism(s) – internal vs. external shocks, baryon fraction, interaction with the environment and propagation questions – and is therefore crucial for eventual understanding of what makes a GRB.

6.2 High-Energy GRB Observations and Astroparticle Physics

The origin of ultra-high-energy cosmic rays has been suggested to be GRBs (Waxman 1995). If bulk Lorentz factors are greater than 100, protons could be accelerated to energies $> 10^{20}$ eV, giving rise to the

highest-energy gamma rays via synchrotron emission. The gamma-ray afterglows would persist for several days and contain an order of magnitude more fluence than the prompt emission (Totani 1998). GLAST should be sensitive enough to detect these afterglows.

Bursts of high-energy gamma rays are a predicted signature of the evaporation of primordial black holes (PBHs). Proof of the existence and evaporation of PBHs would be of fundamental importance to physics and cosmology; in evaporation, PBHs make the transition to a state describable only by quantum gravity. Such “final state” objects have been predicted by both string theories and by quantization of “classical” black holes. Since Hawking radiation (which leads to these states) has never been confirmed, detection of PBHs would be a crucial first step toward experimental contact with theory. Also, the temporal pattern of Hawking radiation has been shown to include possible information on the onset of particle supersymmetry, if it exists (Coyle & Sommerville 1999). Heckler (1997) calculated that the formation of a photosphere will degrade the emitted photons, both primary and secondary, by a typical factor of order 10^3 , resulting in a peak burst flux near 5 GeV, ideally suited for observation with GLAST.

Amelino-Camelia et al. (1998) make the very exciting prediction that GRBs may be able to probe the scale of grand unification and quantum gravity. String theory predicts that space-time is granular at the Planck scale, $\sim 10^{19}$ GeV, and consequently light should suffer an energy-dependent dispersion of order 10 ms $\text{GeV}^{-1} \text{Gpc}^{-1}$. GRBs should have temporal structures comparable to this timescale at energies ~ 10 MeV and above, as they do at lower energies (e.g., Walker et al. 2000).

6.3 Expected GLAST Observations of GRBs

EGRET detected four GRBs above 100 MeV (Fig. 6-3), the brightest that occurred within the field of view of its spark chamber. EGRET also detected 30 GRBs above 1 MeV in its calorimeter. Their spectra are consistent with power-law form, exhibiting no high-energy cutoff, which could mean that most or all GRBs have high-energy emission, but EGRET was not sensitive enough to detect it.

The LAT will detect many more GRBs than EGRET, and many more gamma rays per event. The increased sensitivity is a combination of four factors:

- LAT’s effective area is ~ 6 times that of EGRET and does not fall off above 500 MeV;
- EGRET had a deadtime per gamma ray of ~ 100 ms,

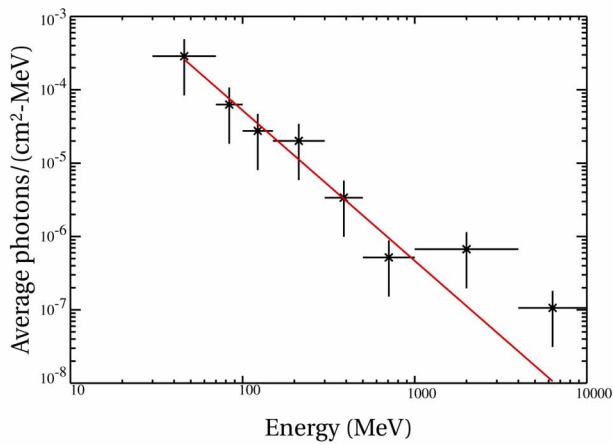


Figure 6-3 Average spectrum measured by EGRET for four bursts – 45 photons > 30 MeV, and 4 photons > 1 GeV. The differential photon spectral index for the fitted line is 1.95 ± 0.25 (Dingus et al. 1998).

comparable to GRB pulse widths at lower energies where time profiles are well characterized, whereas GLAST will not be deadtime limited – this will be essential to detection of gamma rays during brief or intense pulses.

- LAT’s field of view is more than four times that of EGRET – resulting in many more bursts being detected;
- GLAST will be slewed continuously to keep Earth out of its field of view (see §12), which results into a gain of a factor of ~ 2 in observing time.

Figure 6-4 shows the results of a detailed simulation of the number of gamma rays detected by the LAT for the ~ 270 bursts expected within the field of view per year. More than 50 bursts per year will have more than 100 gamma rays above 100 MeV – sufficient signal strength to measure power-law spectral indices with a typical error of 0.1. Source localizations will be smaller than $10'$ (comparable to those of Swift) for ~ 100 GRBs per year, enabling afterglow searches at longer wavelengths and redshift determinations.

Both the LAT and the GBM will measure the spectra of these bursts (Fig. 6-5). The instruments are quite complementary, because of the interrelatedness of the gamma-ray production and attenuation mechanisms. The kinds of temporal variations predicted in Figure 6-1 indicate that the prompt emission has multiple features that are initially only in the gamma-ray energy range. The simultaneous monitoring of these features across the gamma-ray range will be valuable for understanding gamma-ray bursts just as the multiwavelength observations have been so useful for understanding the same types of features in AGN emissions. The difference is that in AGN these features are spread from radio to optical to

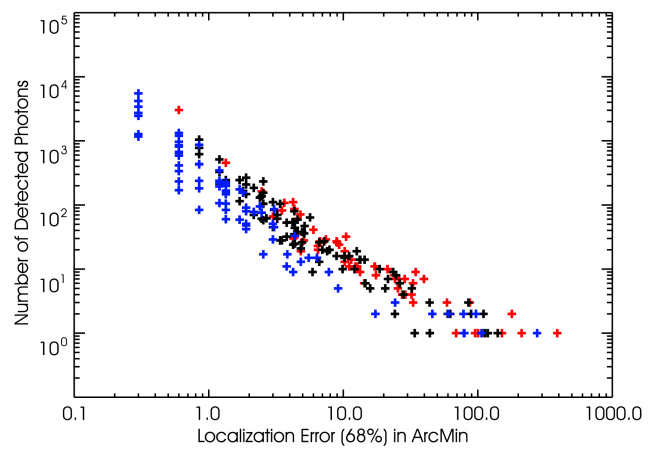


Figure 6-4 Simulation showing the accuracy of location determination for the >200 GRBs per year that will be detected by the LAT. A realistic, discrete distribution of power-law spectral indices was used, based on EGRET spark chamber and TASC detections of GRBs. The points are color coded by spectral index: blue (1.6, 1.8), black (2.0), and red (2.2, 2.4). The simulation uses flux and duration distributions determined by BATSE below 1 MeV, in addition to the power-law indices, to extrapolate the GRB fluences to energies greater than 100 MeV.

X-ray to gamma rays, whereas in GRBs all the prompt, rapidly varying features are in gamma-rays alone.

If quantum gravity effects introduce a dispersion in gamma-ray propagation, simulations indicate that the size of the effect could be detected using only the 20 brightest bursts observed by GLAST in two years, even if the pulses are only 100-ms-wide (Norris & Bonnell 1999). Corroborating the connection to quantum gravity for any dispersion found would require demonstration of the distance dependence of the dispersion.

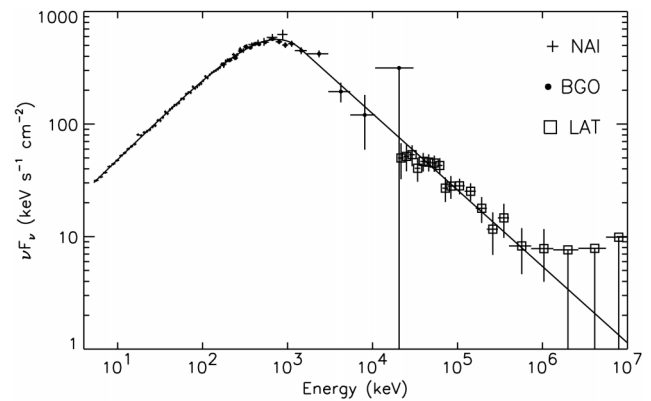


Figure 6-5 Simulation of the spectrum of GRB 940217 as would be observed by the GBM and the LAT. For the GBM, data points from the NaI and BGO detectors are indicated separately.

7. Pulsars

The first astronomical sources detected at gamma-ray energies were pulsars, i.e., rotating, magnetized neutron stars. These neutron stars remain some of the best laboratories for studying extreme physical conditions, including the strongest gravitational forces, largest magnetic fields, and efficient acceleration of some of the highest energy particles in the Universe. Pulsar studies are now done across the full electromagnetic spectrum. Every band contributes to our understanding of these exotic objects, but the gamma-ray band is uniquely important for understanding the basic workings of the pulsar phenomenon. How and where does the particle acceleration take place? What is the shape of the particle beam, and how is its energy converted to photons? What fraction of the sky does a pulsar beam illuminate, and hence how many pulsars are there in the Galaxy and how often are they born? Where does the bulk of the energy go, since it is not seen in the pulsed radiation?

7.1 Gamma-Ray Observations

High-energy gamma-rays represent the bulk of the power output from many pulsars, and gamma-rays are produced by much simpler physical processes than, for example, coherent (nonlinear) radio emission. Gamma-ray beams are relatively large, so a more nearly complete pulsar sample can be studied in that band. The stage has been set by the seven pulsars studied by EGRET (Fig. 7-1), which include the brightest

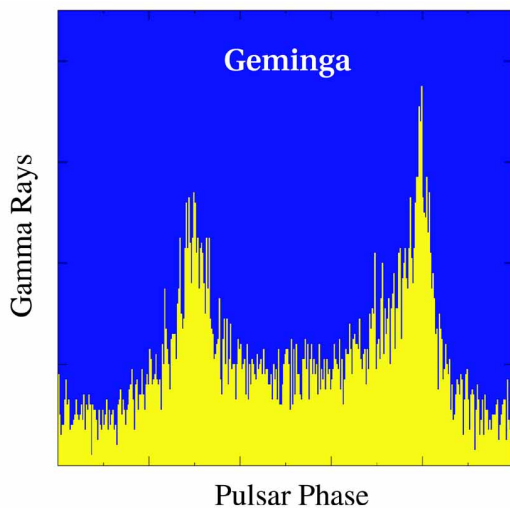


Figure 7-1 Light curve of the Geminga pulsar (period 237 ms) observed by EGRET in gamma rays above 100 MeV.

persistent sources in the gamma-ray sky. In addition, many of the brightest unidentified EGRET sources (54) are coincident with high-mass stars or supernova remnants and are also likely to be associated with pulsars. Thus pulsars could be a dominant constituent of the Galactic gamma-ray sources.

7.2 GLAST and Pulsar Models

Pulsar models make specific, testable predictions for pulsar emissions. Different models make very different predictions for the shape of the pulsar beam, and hence for what fraction of radio pulsars will be seen in gamma rays. With high altitude outer gap accelerators, the beams of young pulsars which are viewed at large angles to the spin axis should be detectable (e.g., Romani 1996). Other models with near-surface polar cap emission (e.g., Harding 1981) predict that gamma-ray visibility is more purely an effect of radiation efficiency (Fig. 7-2).

GLAST will test pulsar emission physics by providing high quality phase-resolved spectra. For the three brightest pulsars, EGRET data already show a complex variation of the gamma-ray spectrum with spin phase. These results challenge pulsar models — but working backward to constrain the underlying physics is very difficult given the small sample and large statistical uncertainties. GLAST will have the sensitivity and resolution to provide detailed spectra

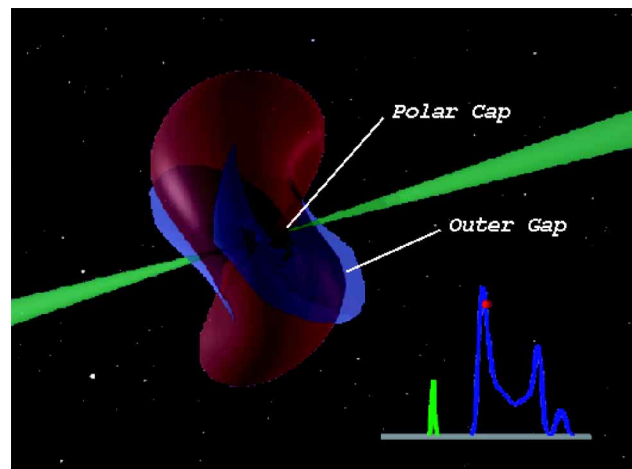


Figure 7-2 Three-dimensional simulation of the Vela pulsar. The spin axis is vertical. The red surface is the closed zone, the polar cap is at the base of the green (radio) beam, and the outer gap surface is in blue. The light curve, calculated for the Outer Gap model, has the same color coding.

for all the EGRET-detected pulsars and more. The models show that the spectral phase variations can be used to reconstruct the pulsar acceleration process and probe the physics of these unique accelerators that produce beams of electrons, positrons and other particles to multi-TeV energies. Multi-GeV sensitivity is particularly important for this work; Figure 7-3 shows how GLAST's vastly improved sensitivity in this regime can use the shape of the high-energy cutoff to discriminate between competing models.

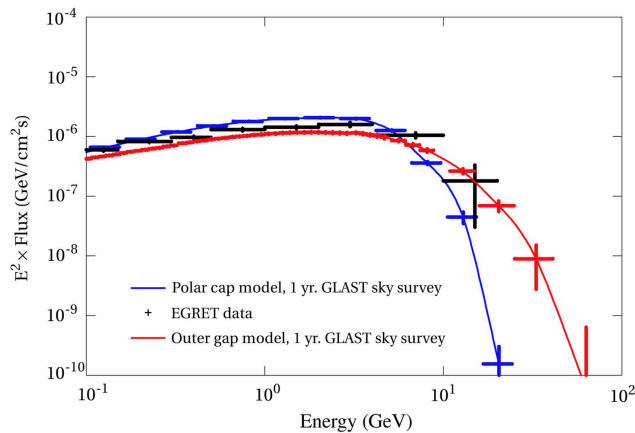


Figure 7-3 Modeled high-energy spectrum of the Vela pulsar. The highest energy EGRET point is based on 4 photons (Thompson et al. 1999). The error bars for the two models (Daugherty & Harding 1996; Romani 1996) are based on a one-year GLAST sky survey. GLAST will clearly distinguish these models at high energies.

GLAST may detect (and study as a function of phase) as many as 250 pulsars, approximately half of which would be previously unknown in the radio (McLaughlin & Cordes 2000 and Fig. 7-4). The predictions are model dependent, but GLAST should produce a large sample of gamma-ray pulsars.

Geminga is the first and most famous example of a radio-quiet pulsar. Additional radio-quiet pulsars, including possible “magnetars” having the strongest magnetic fields yet detected, have been discovered in the hard X-ray band (Vasisht & Gotthelf 1997; Kouveliotou et al 1998). Harding & Zhang (2001, §4) propose that the unidentified, steady, soft-spectrum EGRET sources apparently associated with the Gould Belt could be pulsars viewed outside their radio beams and near the edge of their gamma-ray beams. A careful census of these non-radio pulsars is crucial to understanding the supernova rate and distribution in the Galaxy. Geminga’s pulsations were found in X-rays (Halpern & Holt 1992), and such searches for X-ray pulsation for candidate gamma-ray pulsars will be

feasible for the small GLAST error boxes. But unlike EGRET (see Mattox et al. 1996, Jones 1998), GLAST also has the exciting capability of directly finding pulsations, independent of radio or X-ray results. GLAST will be able to detect pulsations in essentially all of the unidentified EGRET sources, if they are radio-quiet pulsars (McLaughlin & Cordes 2000).

EGRET just scratched the surface of what is to be learned about pulsars from high-energy gamma rays, but the EGRET results allow confident projection to the much higher sensitivity of GLAST. The ability to study more than the brightest handful of sources, and to study bright sources with vastly improved photon statistics, makes GLAST an exciting instrument for pulsar astrophysics.

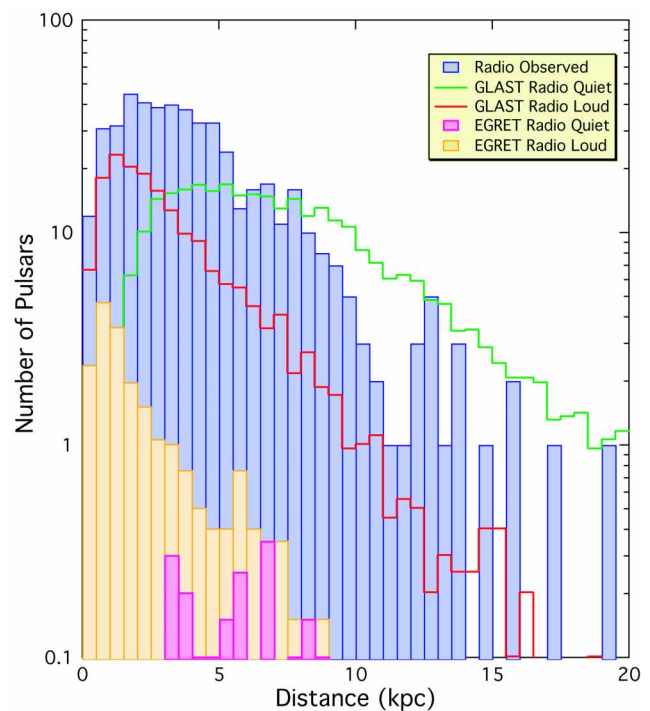


Figure 7-4 Results of a Monte Carlo simulation of galactic pulsars (Gonthier et al. 2000), showing the number of pulsars as a function of distance from Earth that are detectable by radio surveys (blue), and the subsets of those detected radio pulsars that are detectable by EGRET (pink) and by GLAST (red), assuming gamma-ray luminosity predicted by the polar cap model of Zhang & Harding (2000). Also shown are the numbers of radio-quiet pulsars detectable as point sources by EGRET (yellow) and GLAST (green). GLAST will be more sensitive than radio surveys to pulsars at large distances (>5 kpc) and is expected to detect more radio-quiet than radio-loud pulsars in both polar cap and outer gap models.

8. Cosmic Rays and Interstellar Emission

Cosmic rays, relativistic charged particles from space, have been studied since early in the twentieth century. Even so, the question of the origin of cosmic-ray (CR) nuclei remains only partially answered, with widely accepted theoretical expectations but incomplete observational confirmation. GLAST has the potential to be the first instrument to detect the production sites of CR nuclei, long believed to be supernova remnants (SNRs). Through observations of diffuse gamma-ray emission produced by interactions of CRs with interstellar gas and photons, GLAST also will be a powerful instrument for study of the distribution of CRs within the Milky Way and in external galaxies.

Theoretical models and indirect observational evidence support the idea that Galactic CRs are accelerated in the shocks of SNRs with spectra ranging up to about 10 TeV on time scales of order 10^3 – 10^4 yr (Lagage & Cesarsky 1983; Drury et al. 1994; Baring et al. 1999). Later, after the CRs escape from SNRs, they diffuse through relatively small regions of the Galaxy, trapped by the Galactic magnetic fields (Berezinskii et al. 1990). Since CRs gradually leak out of the Galaxy on a time scale of about 20 Myr (Connell et al. 1998) and since the energy content in Galactic CRs is more or less in a state of equilibrium, roughly 10% of the 10^{51} erg of kinetic energy of a SNR must be transferred to CRs to maintain this equilibrium (Parker 1969; Blandford & Eichler 1987; Lingenfelter 1992). Furthermore, because the energy dependence (actually rigidity dependence) of the residence time of CRs in the Galaxy varies as $E^{-0.6}$, and since the differential spectrum of the CRs observed at Earth is proportional to $E^{-2.7}$, the differential spectra of the CRs accelerated by SNRs are expected to be approximately proportional to $E^{-2.1}$.

8.1 Recent Results

Important advances in understanding CRs in the Milky Way were made with EGRET. The detection in the Milky Way of the broad spectral feature at 68 MeV, called the π^0 bump, from the decay of neutral pions produced in nucleon-nucleon interactions (Hunter et al. 1997), provided direct evidence of the presence of CR nuclei (Fig. 8-1). The detection of gamma-ray emission from the Large Magellanic Cloud (LMC, Sreekumar et al. 1992), and the non-detection of gamma-rays from the Small Magellanic Cloud (SMC, Sreekumar et al. 1993) proved that cosmic rays are

galactic, rather than metagalactic or universal: if the CR density in the SMC were as great as in the relatively nearby LMC, it would have been strongly detected by EGRET.

A number of SNRs are reported to be coincident with EGRET sources (e.g., Romero et al. 1999). In general, these SNRs exhibit OH-maser emission (Green et al. 1997), have relatively flat radio spectra (Green 1998), have thermal-composite X-ray morphologies (Rho 1995), and have gamma-ray photon spectra with differential spectral indices of about two, which

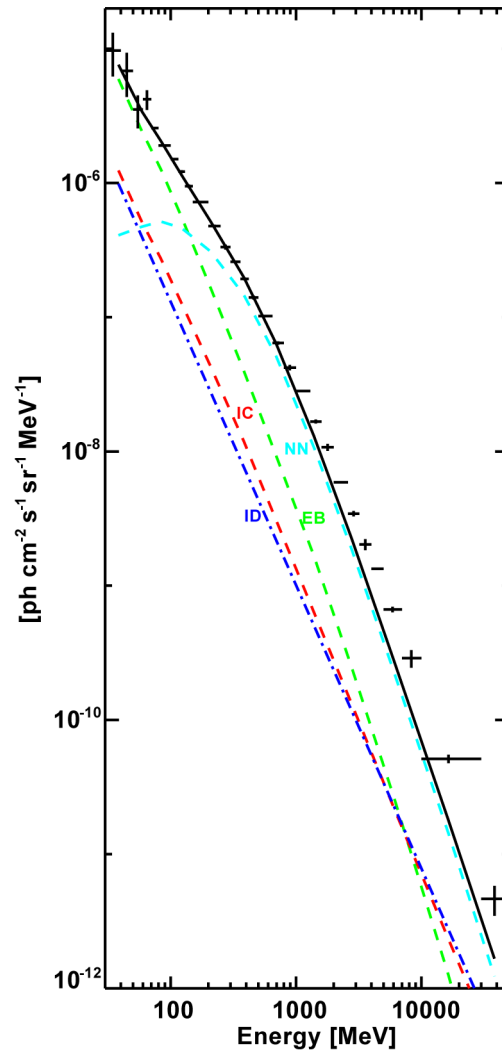


Figure 8-1 Spectrum of the inner Milkyway ($|l| < 60^\circ$, $|b| < 10^\circ$) observed by EGRET (Hunter et al. 1997). The electron-bremsstrahlung (EB), inverse Compton (IC), isotropic diffuse (ID), and π^0 decay (NN, for nucleon-nucleon) components from the model of Hunter et al. (1997) are indicated. The π^0 component is clearly evident.

suggests that the SNRs are interacting with molecular clouds and that the gamma rays are produced by the interaction of CRs with these high-density clouds. However, these results are uncertain because the angular resolution of EGRET is too poor to determine, e.g., whether the sources are actually neutron stars created during supernova explosions rather than diffuse in nature, and because the photon statistics available from EGRET data are insufficient to determine whether the spectra have π^0 features. Furthermore, TeV gamma-ray observations with atmospheric Cherenkov telescopes (§10) indicate that the hard gamma-ray spectra observed in the EGRET energy range may not extend to higher energies (Buckley et al. 1998).

Although the results of the EGRET observations of SNRs are somewhat ambiguous, recent X-ray and TeV gamma-ray observations of SN 1006 (Koyama et al. 1995; Tanimori et al. 1998), and X-ray observations of other young SNRs demonstrate that at least electrons are accelerated to very high energies in the shocks of SNRs. Some of the X-ray emission of these young SNRs seems to be produced by the synchrotron radiation of electrons that have been accelerated to energies of 10–100 TeV or more. On the assumption that CR nuclei are also accelerated in these SNRs, estimates of the total energies of the CR particles appear to be consistent with the total CR energy expected per SNR. Although EGRET did not detect gamma-ray emission from SN 1006, its upper limit for the flux does not exclude the possibility that nuclei are

accelerated to similar energies as the electrons.

One unexpected finding from EGRET was the so-called GeV-excess, a systematic underprediction of the super-GeV intensity by models based on the local spectrum of cosmic rays (e.g., Hunter et al. 1997; Fig. 8-1). This is not due to a calibration error, or an error in the calculation of gamma-ray production (Mori 1997), or unresolved pulsars (Pohl et al. 1997). Pohl & Esposito (1998) pointed out that the effect could be explained by the expected non-uniformity of CR electrons which results from their acceleration near supernova remnants and their relatively rapid energy losses. Their suggestion is that the CR electron spectrum is softer than average in the solar vicinity.

8.2 Advances with GLAST

The conclusive observational signature of CR nuclear acceleration by a SNR would be the π^0 bump from CRs interacting in an interstellar cloud at the shell of the SNR. GLAST offers the prospect of resolving SNR sources, distinguishing shell emission from compact sources of gamma rays (Fig. 8-2), as well as measuring the spectral signature of π^0 decay on top of electron bremsstrahlung and inverse-Compton emission from CR electrons associated with SNRs (see Fig. 8-3 for a minimalist case; nature may provide much more prominent pion bumps in many SNRs).

Detection of the π^0 bump in a SNR-cloud interaction region would also permit the determination

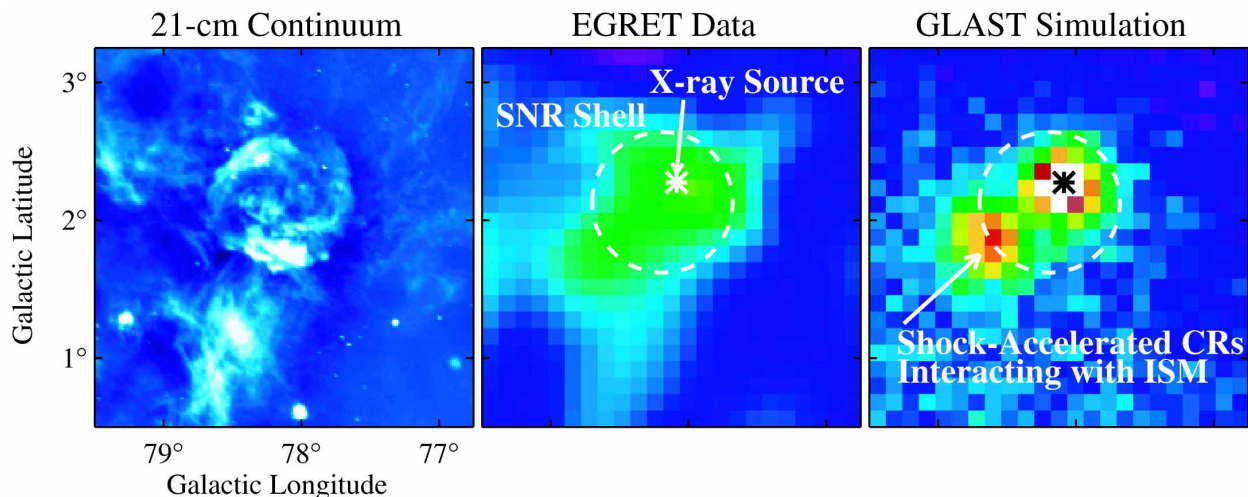


Figure 8-2 Radio continuum emission of the Gamma Cygni SNR at 1.4 GHz from the (Canadian Galactic Plane Survey, English et al. 1998 compared with EGRET observed and GLAST simulated images > 1 GeV. The dashed circles indicate the location of the shell of the SNR (Higgs et al. 1977). An X-ray source suspected to be a gamma-ray pulsar (Brazier et al. 1996) is shown as an asterisk. In the GLAST model of data from a 1-year sky survey, the EGRET flux has been partitioned between the pulsar and a region at the perimeter of the shell where the CRs are interacting with an ambient interstellar cloud.

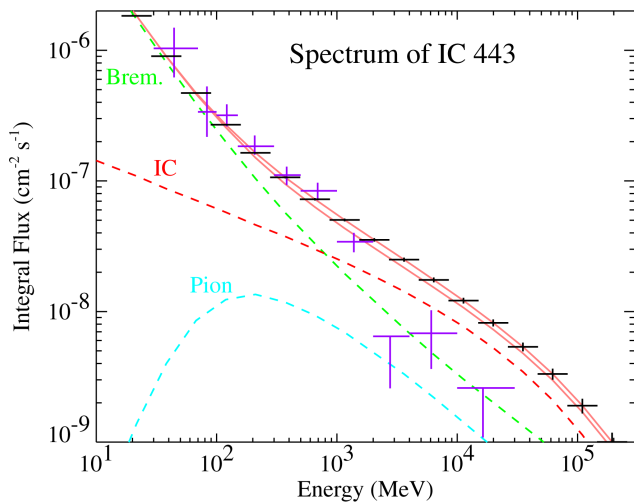


Figure 8-3 Model gamma-ray spectrum for SNR IC 443 adapted from Baring et al. (1999) illustrating how GLAST can detect even a faint π^0 -decay component. The components of the total intensity (upper red curve) are π^0 -decay, inverse-Compton scattering, and electron bremsstrahlung. The lower red curve is the total intensity without π^0 -decay emission. The EGRET data for the source coincident with IC 443 (2EG J0618+2234, Esposito et al. 1996) are indicated in purple and simulated measurements from a 1-year sky survey with GLAST are plotted in black, with 1- σ error bars.

of relative number densities of CR nuclei and electrons. (The spectrum of CR electrons can be determined from models of the nonthermal bremsstrahlung or inverse-Compton gamma-ray emission or of the radio synchrotron emission.) At Earth, the number density of CR nuclei is about one hundred times larger than the density of CR electrons near a kinetic energy of 1 GeV (Meyer 1969). This ratio is also consistent with models of particle acceleration in SNRs (Bell 1978; Baring et al. 1999). Therefore observations with GLAST could provide additional evidence that Galactic CRs are predominantly accelerated in SNRs.

In addition, GLAST observations of remnants such as SN 1006 will measure the inverse-Compton spectra produced by electrons that have energies ~ 0.2 –2 TeV. These data combined with radio (electron energies ~ 1 –10 GeV) and X-ray (electron energies ~ 10 –100 TeV) synchrotron data, will define the broadband electron spectra of the remnants. Collectively, such data will provide a powerful means of testing models of particle acceleration in the shocks of SNRs.

Study of diffuse interstellar emission from the Galactic ridge at energies below 100 MeV with GLAST

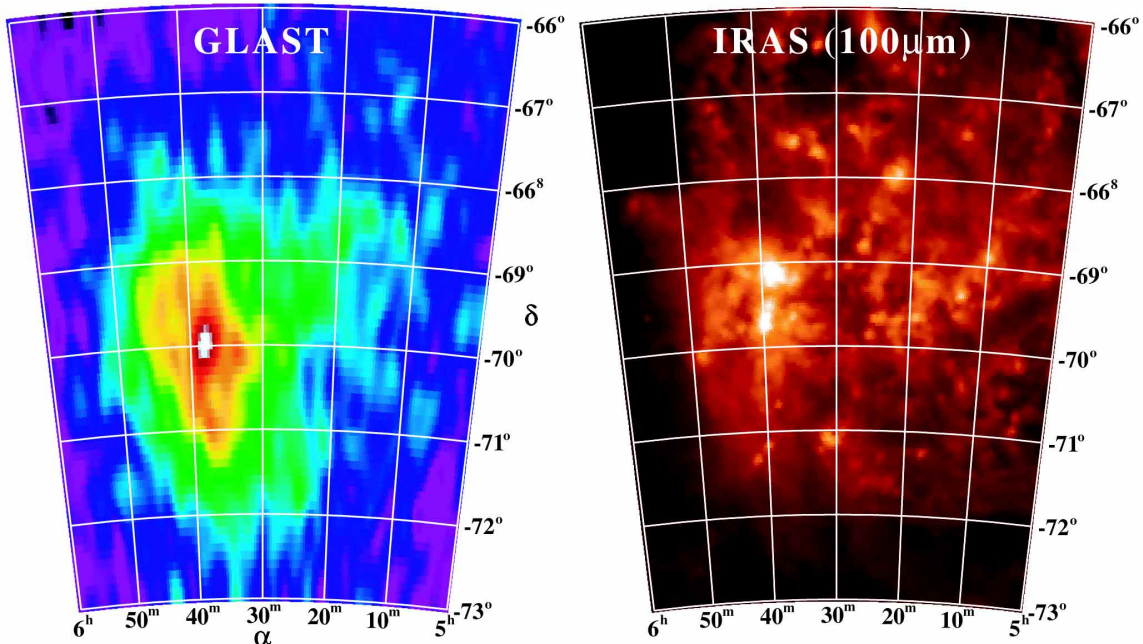


Figure 8-4 Simulated map of the LMC in >100 MeV gamma rays from a one-year sky survey with GLAST together with an IRAS 100 μm map at the same scale. The simulation is based on a model of the LMC by Sreekumar (1999) and also includes foreground diffuse emission from the Milky Way and an isotropic background consisting of a distribution of faint point sources. The infrared map traces the extent of the LMC in massive star formation. GLAST will reveal whether the CR density is enhanced in the enormous 30 Doradus star-forming region, the bright knot of infrared emission in the IRAS map.

may resolve the question of the origin of diffuse hard X-ray emission. Yamasaki et al. (1997) propose that ASCA observations of the inner Galaxy can be explained by continuous production of low-energy cosmic-ray electrons by SNRs.

GLAST will also be able to study CR production and confinement processes in other galaxies. Although the LMC is the only normal galaxy other than the Milky Way that has been detected with EGRET (as an unresolved source), GLAST should resolve gamma-ray emission from the LMC (Fig. 8-4) and other Local Group galaxies, such as the SMC and M31 (Fig. 8-5), and should easily detect starburst galaxies, such as NGC 253 and M82 (Blom et al. 1999). Resolving spectral variations in, say, the LMC, would increase confidence in the explanation of the GeV excess observed in the Milky Way (§8.1).

GLAST will also advance understanding of the dense interstellar medium. The diffuse gamma-ray emission from interstellar clouds illuminated by CRs has proven to be one of the most direct and reliable tracers of their masses. Dense, star-forming interstellar clouds are largely cold H_2 , which is very difficult to detect directly. The 2.6-mm line emission from the $J = 1-0$ rotational transition of CO is a widely-observed

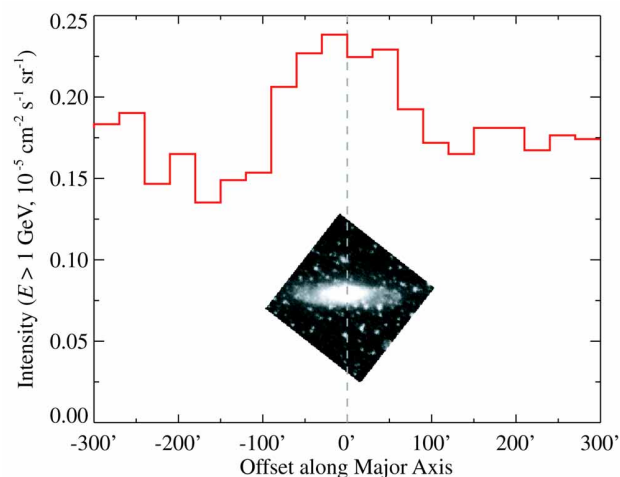


Figure 8-5 Simulated intensity profile of M31 for >1 GeV gamma rays from a two-year sky survey with GLAST together with an optical image at the same angular scale. The intensity profile was derived from a model for the diffuse gamma-ray emission of M31 itself, along with foreground Galactic diffuse emission and faint background point sources. The emission model for M31 was derived from the distribution of interstellar gas (Dame et al. 1993) and an assumed flux of $1.0 \times 10^{-8} \text{ cm}^{-2} \text{ s}^{-1}$ ($> 100 \text{ MeV}$), consistent with the upper limit of Blom et al. (1999).

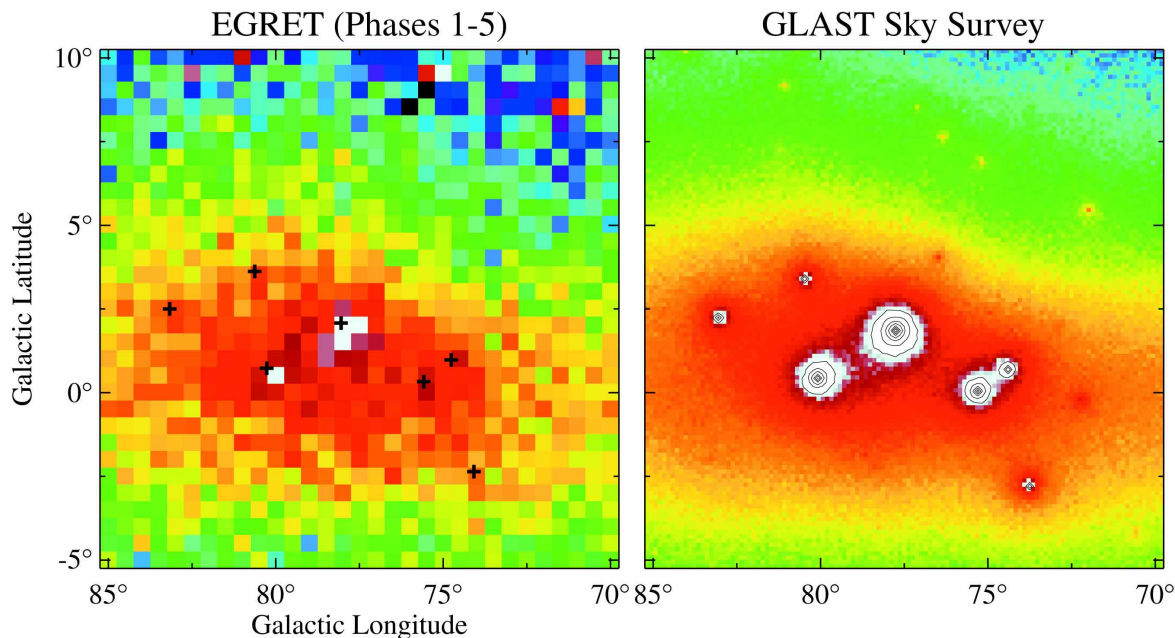


Figure 8-6. Diffuse gamma-ray emission and point sources near the plane in Cygnus comparing EGRET observations with GLAST simulation ($> 100 \text{ MeV}$). In confused regions like Cygnus, several EGRET point sources are seen against massive molecular clouds that may be a spur of a spiral arm viewed end on. The simulated GLAST image is for a 1-year sky survey. The bright point sources are assumed to be the same as in the 3EG catalog (Hartman et al. 1999, indicated with crosses) and the diffuse emission is assumed to follow the model of Hunter et al. (1997). GLAST will likely resolve much more structure in the diffuse emission and better determine the number and position of the embedded point sources.

indirect tracer of molecular hydrogen, and gamma-ray observations are useful for calibrating the relationship between CO and H₂.

The low instrumental background of EGRET made it the first gamma-ray telescope to be well suited to these studies, but the poor angular resolution and statistics have limited the number of regions that can be studied to a few nearby clouds, notably Ophiuchus (Hunter et al. 1994), Orion (Digel et al. 1995; Digel et al. 1999) and massive clouds in the Perseus arm (Digel et al. 1996), the next spiral arm outward from the solar circle. With GLAST data, spatial variations of CR flux (i.e., spatial variations of gamma-ray spectra) will be distinguishable from variations in the column density of gas for the first time on angular scales smaller than

9. Solar Flares

Since the early 1970s solar flares have been known to produce gamma rays with energies greater than several MeV. The production of gamma-rays is understood to involve flare-accelerated charged-particle interactions with the ambient solar atmosphere (see, e.g., Ramaty & Murphy 1987; Hua & Lingenfelter 1987). Bremsstrahlung from energetic electrons accelerated by the flare or from the decay of π^{\pm} secondaries produced by nuclear interactions yields gamma rays with a spectrum that extends to the energies of the primary particles. Proton and heavy ion interactions also produce gamma rays through π^0 decay, resulting in a spectrum that has a maximum at 68 MeV and is distinctly different from the bremsstrahlung spectrum.

The processes that accelerate the primary particles are not well known. Two that have been discussed frequently in the literature are stochastic acceleration through MHD turbulence and shocks (Ryan & Lee 1991; Forman et al. 1986). Particle acceleration is thought to occur in association with large magnetic loops that are energized by flares. For most flares the particles are trapped in a loop and their interactions near the loop footprint generate gamma rays (Mandzhavidze & Ramaty 1992a,b).

9.1 EGRET Observations

EGRET observed very intense flares that occurred in June, 1991. The emission continued for several hours, and photons with energies ranging up to 2 GeV were detected (Kanbach et al. 1993; Schneid et al. 1993; Fig. 9-1). The long durations and high energies led to

molecular clouds.

On larger scales, GLAST will help untangle the diffuse emission from point sources (Fig. 8-6). Estimates based on EGRET data suggest that unresolved pulsars, for example, could account for ~10% of the diffuse intensity above 100 MeV (Hunter et al. 1997; Pohl et al. 1997; McLaughlin & Cordes 2000).

In summary, GLAST will (1) prove whether or not Galactic CR nuclei are predominantly accelerated in SNRs, (2) determine the shape of the CR spectra, (3) determine if similar CR processes are at work in other galaxies, and (4) offer a unique contribution to the study of the interstellar medium of the Milky Way.

speculation that particles either were impulsively accelerated and then efficiently stored in the loop, or they were accelerated for several hours. Spectral features suggest that both primary electrons and protons were involved. Moreover, the time evolution of the spectrum suggests continuous acceleration, since the electron component was so long lived.

Whether all flares produce emission with extended durations is not known. In fact it has been suggested that only flares larger than some threshold exhibit long-duration emission. This conjecture is based on the idea that in a large coronal loop, the time for the diffusion of energetic particles out of the loop is comparable to the acceleration time by stochastic acceleration through MHD turbulence in the loop. Unless the loop is sufficiently large, the particles diffuse out the sides before attaining sufficient energy to create pions.

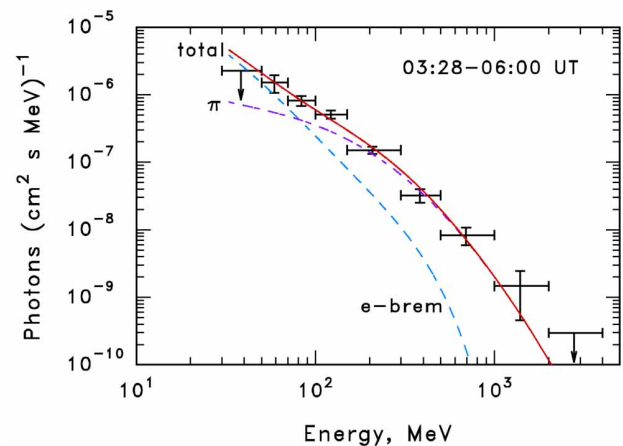


Figure 9-1 The extraordinary solar flare of June 11, 1991 was the best example observed by EGRET.

9.2 Contributions from GLAST

GLAST will contribute in several ways to resolving the questions about where the acceleration takes place and the processes involved. For large flares with high-energy emission extending to 1 GeV, GLAST will be able to image the sites of the acceleration to less than 5', which will reveal whether they are point-like or extended. (The loop size is often comparable to the solar radius.) GLAST's sensitivity to much smaller solar events will reveal if they produce the same long-duration emission as the large events.

LAT's sensitivity and dynamic range offer significant improvements for studying flare spectra and their time evolution. Electrons with energies as great as 50 MeV are not uncommon, but the emission from these particles tends to be short-lived in many flares. The gamma-ray spectrum in this case is a power law from bremsstrahlung interactions. A sharp break in the spectrum would be strong evidence for an acceleration mechanism involving electric fields. If protons are accelerated, the spectra will have evidence of a π^0 bump at 68 MeV. Since the rate of energy loss by electrons is much larger than for protons, the relative time scales of electron and π^0 spectral variations indicates whether trapping or extended acceleration is responsible for long-duration flares.

Instrumental deadtime has an important impact on studies of solar flares, because the flares can be intense. The initial spikes in the June, 1991 flares completely saturated the EGRET anticoincidence system for hours (Fig 9-2). GLAST will have much greater immunity from saturation, with a deadtime three orders of magnitude less than EGRET, and will be able to study the initial, impulsive phase of flares. (For particularly intense flares, special operating modes may need to be established even for GLAST to limit the rate of triggers from gamma rays and to mitigate the effect of hard X-

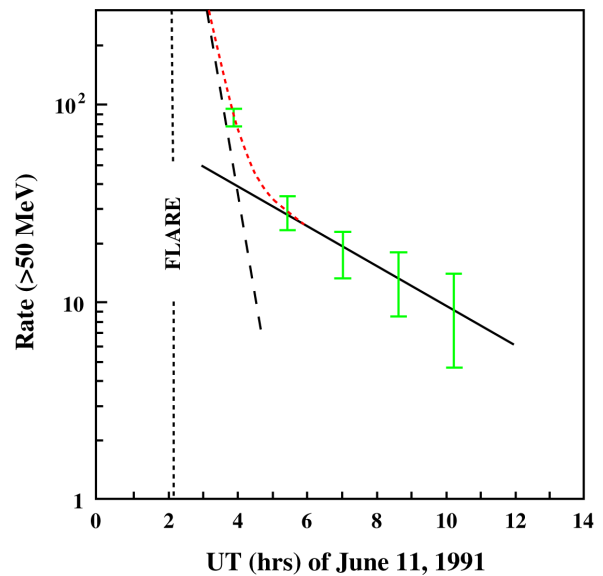


Figure 9-2 Initial spikes in the June 1991 flares completely saturated the EGRET anticoincidence system for hours (Kanbach et al. 1993).

rays interacting in the ACD (§11). Turning off the outer towers and the upper detector layers of the towers are being considered.)

The GBM will provide wider field-of-view monitoring of solar flares, and permit study of the evolution of flares simultaneously across the several keV-GeV energy range. It will also detect nuclear line emission from cosmic rays accelerated in flares.

GLAST will be launched near the minimum of the solar cycle, and the frequency and intensity of solar flares will increase throughout most of the planned five-year mission. If the goal of a 10-year mission life is achieved, GLAST will operate for nearly the entire duration of solar cycle 24 (Fig 9-3). During this time, GLAST will be the only high-energy observatory to complement several solar missions at lower energies: STEREO, Solar-B, and Solar Probe.

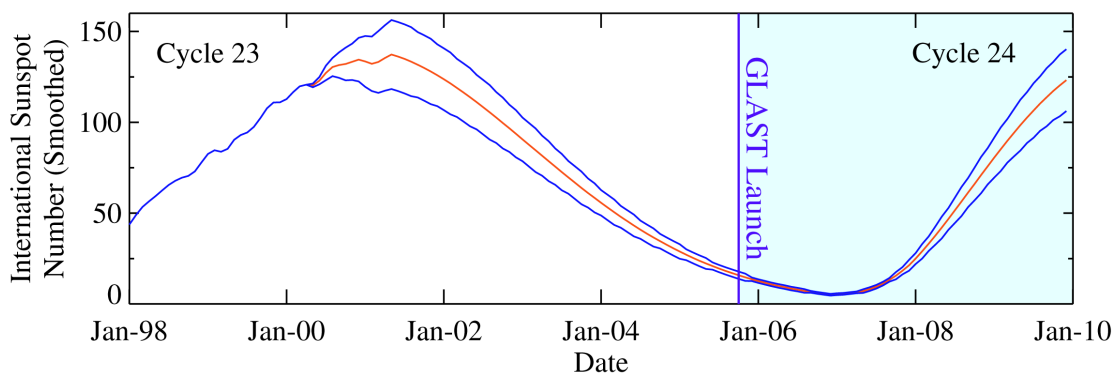


Figure 9-3 GLAST will be able to study solar flares throughout Cycle 24. The sunspot predictions were made by IPS Radio and Space Services (<http://www.ips.gov.au/>). The estimated uncertainties are indicated.

10. Complementarity with Ground-Based Experiments

High-energy gamma rays can be observed from the ground by experiments that detect the air showers they produce in the upper atmosphere. Air shower arrays directly detect the particles (electrons, muons, and photons) in air showers, and atmospheric Cherenkov telescopes (ACTs) detect the Cherenkov radiation created in the atmosphere and beamed to the ground.

In the last decade, ground-based Cherenkov telescopes have made great progress, both in technical and scientific terms. (For a recent review, see Ong 1998.) On the technical side, atmospheric Cherenkov telescopes have demonstrated that a high degree of gamma/hadron discrimination and a source location accuracy of $10'–30'$ (depending on the source strength) can be achieved based on the detected Cherenkov image. The Crab nebula, which has been shown to be a standard candle source at very high energies, can be detected with high statistical confidence in less than twenty minutes of observation. The single-photon angular resolution achieved by the state-of-the-art ACTs such as Whipple, CANGAROO, CAT, and HEGRA approaches 0.1° above 500 GeV.

The technical advances in ACTs have led to important scientific results. Now at least seven gamma-ray point sources have been detected with high statistical significance at energies above 250 GeV. These sources include three pulsar nebulae (Crab, Vela, and PSR B1706-44) and four extragalactic AGNs of the BL Lac class (see §3). Recently, a tentative detection of the supernova remnant SN 1006 was reported (Tanimori et al. 1998); if confirmed, this result could be important for understanding the origin of cosmic rays (§8).

The field of ground-based gamma-ray astronomy is growing quickly and a number of new experiments are under construction or in the proposal stage. MILAGRO is a large, water Cherenkov detector that is the first air shower array to operate at energies below 1 TeV (Atkins et al. 2000). Beginning initial operations in 1999, MILAGRO is making the first all-sky survey at very high energies. The STACEE (Chantell et al. 1998) and CELESTE (Quebert et al. 1997) experiments use large heliostat mirrors at solar energy facilities to collect a much larger fraction of the Cherenkov radiation in gamma-ray air showers than conventional Cherenkov telescopes. The large collection areas may allow these experiments to make ground-based observations in the range 50 GeV to 250 GeV. Both observatories have detected the Crab and their

collecting areas are being increased.

Several major new facilities are under development. These new Cherenkov telescopes are built on the successful tradition of the Whipple, CAT, CANGAROO, and HEGRA experiments. Three such telescopes, designed as arrays of 10-meter class mirrors with fine pixelized imaging cameras, are in the development stage: VERITAS (Bond et al. 2000) in the northern hemisphere and HESS (Kohnle et al. 1999) and CANGAROO-III (Mori et al. 2000) in the southern hemisphere. Another observatory, MAGIC, planned to begin operations in summer 2001 at La Palma on the Canary Islands, will consist of a single 17-m mirror (Martinez et al. 1999). Construction of HESS started in August, 2000, and operations with limited capability are expected to begin in 2002. Construction of CANGAROO-III started in April, 1999, and the instrument is expected to be fully operational in 2004. Figure 10-1 shows a comparison of sensitivities of the various instruments.

Ground-based detectors, particularly the imaging Cherenkov telescopes have very large collection areas ($>10^8$ cm²), excellent angular resolution, and good energy containment at very high energies (26 radiation lengths). Owing to their large collection areas, they have the capability of detecting very short flares from known sources, e.g., variations on 15-minute timescales in Mrk 421 (Gaidos et al. 1996). These detectors also have limitations, including low duty cycles (10%), small fields of view ($<5^\circ$), systematic energy and sensitivity calibration uncertainties, and poor capabilities for observations of extended, randomly located, rapidly flaring events (e.g., gamma-ray bursts), or diffuse sources.

In contrast, GLAST has a very large field of view, high duty cycle, and a wide energy range from 20 MeV to 300 GeV with excellent energy resolution and low systematic energy calibration uncertainties. Thus, GLAST will operate in fundamentally complementary manner. GLAST will provide the ground-based observers with alerts for transient sources (§11), and the new imaging Cherenkov telescopes are being built to slew within a few tens of seconds following notification. GLAST's observations of steady sources at the highest energies will be used to reduce the systematic errors in the sensitivities of the ground-based observatories.

For individual point sources, ground-based instruments have unparalleled sensitivity at very high

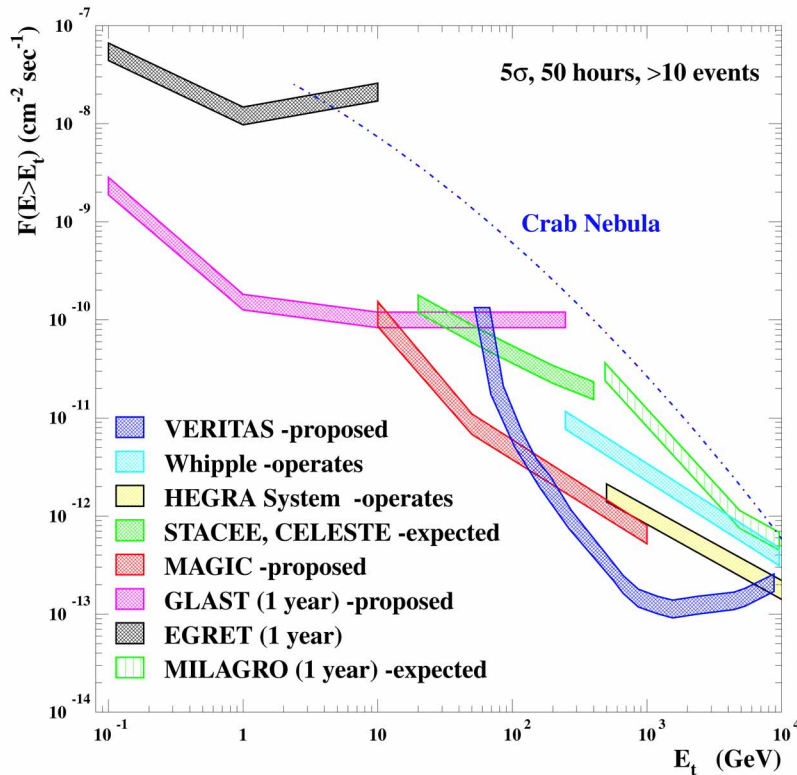


Figure 10-1 The predicted sensitivities of a number of operational and proposed ground-based Cherenkov telescopes for a 50-hour exposure on a single source. EGRET, GLAST, and MILAGRO sensitivities are shown for one year of all-sky survey. HESS is projected to have a threshold of 40 GeV and a sensitivity approximately 10 times greater than HEGRA. Note the excellent overlap region between GLAST and future Cherenkov telescopes, which will allow accurate energy and sensitivity calibrations to be made for the ground-based instruments in the 50–500 GeV energy range, for example via contemporaneous observations of the Crab Nebula.

energies (above 50–250 GeV), with the ability to resolve shorter-duration flares. For many objects, full multiwavelength coverage over as wide an energy range as possible will be needed to understand the acceleration and gamma-ray production mechanisms. In addition, at energies above ~10 GeV the spectra from distant AGNs may be cut off due to absorption by the extragalactic background light (§3). Spectral measurements by both GLAST and ground-based instruments will be needed to measure these absorptive effects accurately and so measure the spectrum of the

EBL from microwave to optical wavelengths.

In summary, ground-based gamma-ray experiments study a number of astrophysical sources that are of relevant to the scientific goals of GLAST, and in a complementary manner. These experiments have made significant progress over the last ten years. The success and continued development of the ground-based very high-energy gamma-ray astronomy greatly enhance the scientific merits and rationale for GLAST and vice versa.

11. Instrument Development

11.1 Large Area Telescope

The primary interaction of photons in the GLAST energy range with matter is pair conversion. This process forms the basis for the underlying measurement principle by providing a unique signature for gamma rays, which distinguishes them from charged cosmic rays whose flux is as much as 10^5 times larger, and allowing a determination of the incident photon directions via the reconstruction of the trajectories of the resulting e^+e^- pairs.

This technique is illustrated in Figure 11-1. Incident radiation first passes through an anticoincidence shield, which is sensitive to charged particles, then through thin layers of high-Z material called conversion foils. Photon conversions are facilitated in the field of a heavy nucleus. After a conversion, the trajectories of the resulting electron and positron are measured by particle tracking detectors, and their energies are then measured by a calorimeter. The characteristic gamma-ray signature in the LAT is therefore (1) no signal in the anticoincidence shield, (2) more than one track starting from the same location within the volume of the tracker, and (3) an electromagnetic shower in the calorimeter.

The baseline LAT is modular, consisting of a 4×4 array of identical towers (Fig. 11-2). Each $40 \times 40 \text{ cm}^2$ tower comprises a tracker, calorimeter and data acquisition module. The tracking detector consists of 18 xy layers of silicon strip detectors. This detector technology has a long and successful history of application in accelerator-based high-energy physics,

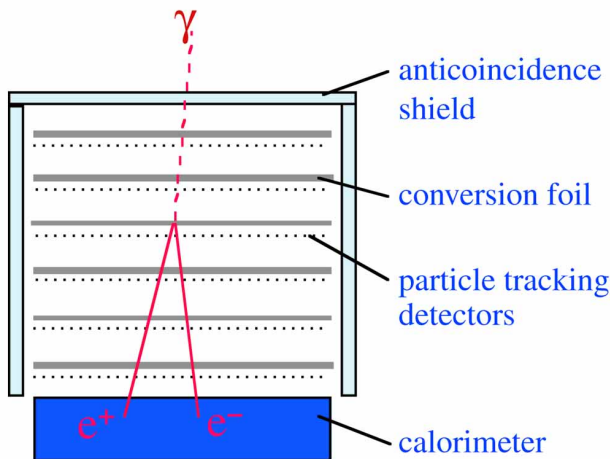


Figure 11-1 Principle of a pair conversion telescope.

and is well-matched to the requirements of high detection efficiency ($>99\%$), excellent position resolution ($<60 \mu\text{m}$ in this design), large signal:noise ($>20:1$), negligible cross-talk, and ease of trigger and readout with no consumables. The calorimeter in each tower consists of 8 layers of 12 CsI bars in a hodoscopic arrangement, read out by photodiodes, for a total thickness of 10 radiation lengths. Owing to the hodoscopic configuration, the calorimeter can measure the three-dimensional profiles of showers, which permits corrections for energy leakage and enhances the capability to discriminate hadronic cosmic rays. The anticoincidence shield, which covers the array of towers, employs segmented tiles of scintillator, read out by wavelength-shifting fibers and miniature phototubes. Basic specifications for the LAT are given in Table 11-1.

The instrument design is based on detailed computer simulations, validated with tests of prototype

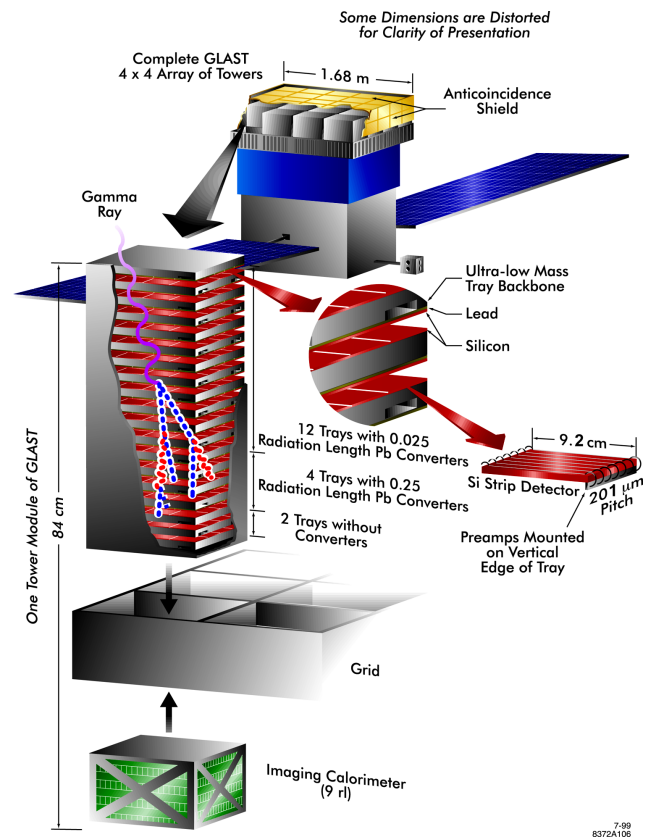


Figure 11-2 The LAT instrument, exploded to show the detector layers in a tower, the stacking of the CsI logs in the calorimeter, and the integration of the subsystems.

Table 11-1 LAT and GBM Resource Requirements

	LAT	GBM
Mass	2600 kg	55 kg
Power	520 W	18 W
Telemetry Rate (Avg.)	300 kbps	4 kbps (9 kbps if triggered data)

towers at particle accelerators. A complete software model of the instrument, including gaps, uninstrumented structural material, noise, inefficiencies and other real-world effects, was constructed using the object-oriented C++ GISMO toolkit. The computer model was used to generate simulated instrument data, and then to develop realistic reconstruction algorithms. The simulations were used to (1) demonstrate the necessary background rejection performance of the instrument, (2) produce realistic triggering and readout schemes, and (3) evaluate and optimize the performance of the instrument (effective area, angular resolution, etc.) after all background rejection cuts and instrumental effects have been taken into account. Accelerator tests of increasingly sophisticated prototype towers were made at the Stanford Linear Accelerator Center (1997 and 1999/2000) and the European Organization for Nuclear Research (CERN) in 1999.

The LAT is self triggered; events that cause detector hits in three planes automatically trigger readouts of each tower and the anticoincidence system. Efficient rejection of the charged particle background, which is thousands of times more intense than the celestial gamma-ray radiation, is essential for GLAST to function. (On-orbit, the expected raw trigger rate will average a few kHz, and the rate of celestial gamma rays will be a few Hz.) The anticoincidence system is only the first line of defense in identifying cosmic rays that trigger the telescope. As described above, from simulations, other discriminators against charged particles have been developed to further reduce the background level. Some of the discriminators will be applied onboard to reduce the trigger rate to the ~30 Hz rate that can be stored and downlinked (§12).

11.2 GLAST Burst Monitor

The GBM will include two sets of detectors: twelve sodium iodide (NaI) scintillators, each 12.7 cm in diameter by 1.27 cm thick, and two cylindrical bismuth germanate (BGO) scintillators, each 12.7 cm in diameter and 12.7 cm in height. A schematic mounting scheme is shown in Figure 11-3, and basic

specifications are given in Table 11-1. (The actual configuration will be finalized when the spacecraft has been selected; §12.2.) The NaI detectors are sensitive in the lower end of the energy range, from a few keV to about 1 MeV and provide burst triggers and locations. The BGO detectors cover the energy range ~150 keV to ~30 MeV, providing a good overlap with the NaI at the lower end and with the LAT at the high end.

GRBs will be detected by a significant change in count rate in at least two of the NaI scintillators; the trigger algorithm will be programmable. Time-tagged event data (with 5 μ s resolution) will be recorded continuously to provide ~50 s of pretrigger information for GRBs. After a trigger, the GBM processor will calculate preliminary position and spectral information for telemetry to the ground and possible autonomous repointing of GLAST. The GBM is projected to detect ~200 GRBs per year.

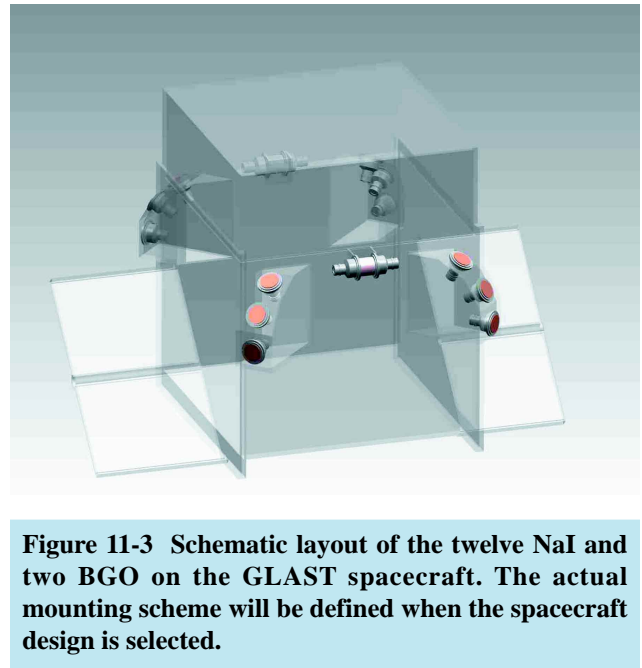


Figure 11-3 Schematic layout of the twelve NaI and two BGO on the GLAST spacecraft. The actual mounting scheme will be defined when the spacecraft design is selected.

12. Mission Overview

12.1 Operations

GLAST is planned for launch in September 2005 and has a design lifetime of five years, with a goal of ten years for operations. After initial operational checkout, the first year of the mission will be devoted to a scanning, all-sky survey. For the remainder of the mission, GLAST will make pointed observations. The observing program, with targets selected by peer review of guest observer proposals, will be uploaded to the spacecraft.

To optimize observing efficiency during the sky survey, the instrument will be pointed in the zenith direction and rocked north-south periodically by $\sim \pm 35^\circ$ to cover the poles of the orbit and east-west to fill in observing gaps around the South Atlantic Anomaly. In this way, the entire sky will be surveyed every two orbits and the exposure will be quite uniform, even on time scales as short as one day. During the pointed phase of the mission, targets will be multiplexed to the extent possible in order to minimize the time lost to earth occultation.

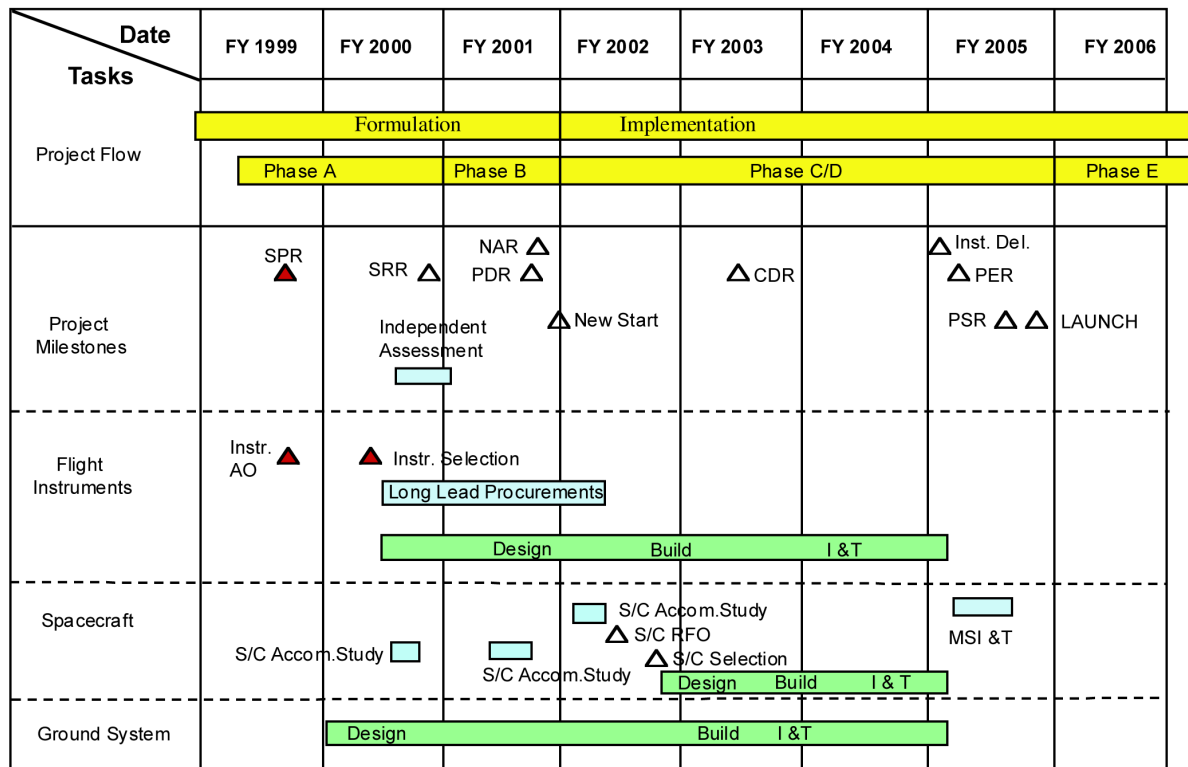
Throughout the mission, autonomous and commanded pointings will be supported for slewing toward GRBs detected onboard and for observing targets of opportunity declared from the ground. For GRBs, the slewing requirements and durations are still being defined.

At the end of operational life, the observatory will undergo a controlled reentry for safe ocean disposal.

12.2 Development Schedule

The high-level development schedule for GLAST is shown in Figure 12-1. The Mission Concept Review (September 1998) and System Requirements Review (September 2000) have been passed. The Non-Advocate Review scheduled for summer of 2001 will begin the approval process for a NASA new start. The ongoing instrument development leads the spacecraft development. Spacecraft development begins in FY 2002, allowing a 3-year development, integration, and test phase.

GLAST Development Schedule



November 2000

Figure 12-1 Highlights of the GLAST development schedule.

12.3 Organization

Overall mission management is being provided by NASA/GSFC. The LAT is managed at Stanford University/Stanford Linear Accelerator Center and is a joint development with NASA, Department of Energy (DOE), and international organizations. The Science Working Group that advises the project on science and operations issues includes representatives from the LAT and GBM teams, DOE, NASA, international institutions, and interdisciplinary scientists selected by competitive proposals.

The principal investigator of the LAT is Peter Michelson (Stanford University). Within the U. S., the principal institutions participating in the development of the LAT are Stanford University/Stanford Linear Accelerator Center, which besides managing the project will be responsible for the integration and testing of the instrument, University of California, Santa Cruz, which is managing the design and construction of the tracker, NASA/GSFC, which is responsible for the anticoincidence detector, the US Naval Research Laboratory, which is contributing to the design of the calorimeter, and Sonoma State University, which is leading the education and public outreach effort. The international partners are France (with contributions to the design and construction of the calorimeter), Japan (Si strip detectors), Italy (tracker assembly), and Sweden (CsI logs for the calorimeter). Institutions participating in the LAT collaboration are listed in Table 12-1.

The principal investigator of GBM is Charles Meegan (NASA/MSFC). The co-PI is Giselher Lichti (Max-Planck-Institut für extraterrestrische Physik, Germany). Institutions participating in the development of the GBM are NASA/MSFC, the University of Alabama in Huntsville, and the Max-Planck-Institut für extraterrestrische Physik, which is providing the NaI and BGO detectors.

The Science Support Center (SSC) for GLAST will be located at NASA/GSFC. The SSC will support the guest observer program and provide public access to GLAST data products, analysis software, and proposal preparation tools such as observation simulators. The operation of the SSC will be overseen by a GLAST Users Group representative of the high-energy astrophysics and particle physics communities.

12.4 Launch Vehicle and Spacecraft

The launch vehicle used for design is the Delta 2920 with a 10-foot fairing. GLAST will be launched from

Agenzia Spaziale Italiana (Italy)
Centre d'études nucléaires de Bordeaux
Gradignan (France)
Collège de France (France)
Commissariat à l'Énergie Atomique (France)
Ecole Polytechnique (France)
Hiroshima University (Japan)
Institut National de Physique Nucléaire et de
Physique des Particules (France)
Institute for Cosmic-Ray Research (Japan)
Institute for Space and Astronautical
Science (Japan)
Istituto di Fisica Cosmica – CNR (Italy)
Istituto Nazionale di Fisica Nucleare (Italy)
NASA/Goddard Space Flight Center
Royal Institute of Technology (Sweden)
Sonoma State University
Stanford University/Stanford Linear
Accelerator Center
Stockholms Universitet (Sweden)
Texas A&M University-Kingsville
U. S. Naval Research Laboratory
University of California, Santa Cruz
University of Rome (Italy)
University of Tokyo (Japan)
University of Trieste (Italy)
University of Washington

Table 12-1 Institutions Participating in the LAT collaboration.

the Kennedy Space Center into a 28.5° inclination, 550 km altitude circular orbit (for which the 2920 has a 4460 kg mass to orbit capability).

The spacecraft will provide both communications at both S-band and X-band frequencies. The S-band system will have nearly-omnidirectional coverage to support communications with the ground for command uplinks and with the Tracking and Data Relay Satellite System for sending alerts about transient sources and receiving target of opportunity commands. Science and housekeeping data will be accumulated in a 50-Gbit solid state recorder and downlinked daily to a shared ground station using X-band with a gimbaled high-gain antenna. An onboard solid-state recorder will have capacity for 36 hours of flight data.

Absolute time (to better than 10 ms) and precision determination of orbit position will be provided by Global Positioning System receivers. Star trackers will provide pointing knowledge to 10'' (1- σ radius) even while the spacecraft is slewing for the sky survey.

References

- Amelino-Camelia, G., et al. 1998, *Nature*, 393, 763
- Ashman, K. M. 1992, *PASP*, 104, 1109
- Atkins, R. et al. 2000, *Nucl Inst Meth A*, 449, 479
- Baring, M. G., & Harding, A. K. 1997, *ApJ*, 491, 663
- Baring, M. G., et al. 1999, *ApJ*, 513, 311
- Begelman, M. C., Blandford, R. D., & Rees, M. J. 1984, *RMP*, 56, 255
- Bell, A. R. 1978, *MNRAS*, 182, 147
- Berezinskii, V. S. et al. 1990, *Astrophysics of Cosmic Rays*, (Amsterdam: North-Holland)
- Bergström, L., & Ullio, P. 1997, *Nucl. Phys B* 504, 27
- Bergström, L., Ullio, P., & Buckley, J. H. 1998, *Astropart. Phys.* 9, 137; referred to as BUB in text
- Bern, Z., Gondolo, P., & Perelstein, M. 1997, *Phys.Lett. B* 411, 86
- Bignami, G. F., et al. 1979, *ApJ*, 232, 649
- Blandford, R., & Eichler, D. 1987, *Phys. Rep.*, 154, 1
- Blandford, R. D., & Königl, A. 1979, *ApJ*, 232, 34
- Blandford, R. D., & Levinson, A. 1995, *ApJ*, 441, 79
- Blandford, R. D., & Rees, M. J. 1978, in *Pittsburgh Conference on BL Lac Objects*, ed. A. M. Wolfe (Pittsburgh: Univ. Pittsburgh Press), 328
- Blazewski, M., et al. 2000, *ApJ*, in press
- Blom, J. J., Paglione, A. D., & Carramiñana, A. 1999, *ApJ*, 516, 744
- Bond, I. H., et al. 2000, VERITAS proposal to DOE NSF (unpublished)
- Bonnell, J. T., et al. 1998, *AIP Conf Proc*, 428, 884
- Böttcher, M. 1999, *ApJ*, 515, L21
- Böttcher, M., & Dermer, C. D. 1998, *ApJ*, 499, L131
- Brazier, K., et al. 1996, *MNRAS*, 281, 1033
- Buckley, J. H. et al. 1998, *A&A*, 329, 639
- Catanese, M., et al. 1997, *ApJ*, 487, L143
- Chantell, M. C., et al. 1998, *Nucl. Inst. Meth. A* 408, 468
- Chiang, J., & Mukherjee, R. 1998, *ApJ*, 496, 752
- Chiang, J., et al. 1995, *ApJ* 452, 156
- Condon, J. J., et al. 1996, *ApJS*, 103, 81
- Connell, J. J., DuVernois, M. A., & Simpson, J. A. 1998, *ApJ*, 509, L97
- Costa, E., et al. 1997, *Nature*, 387, 783
- Coyne, D., & Somerville, R. 1999, in *Proc. UCLA Dark Matter Conf.*, *Physics Reports*, in press
- Dame, T. M., et al. 1993, *ApJ*, 418, 730
- Daugherty, J. K., & Harding, A. K. 1996, *ApJ*, 458, 278
- Dermer, C. D. 1997, *Proc. 4th Compton Symposium*, ed. C. D. Dermer, M. S. Strickman, & J. D. Kurfess (New York: AIP), 1275
- Dermer, C. D., Chiang, J., & Böttcher, M. 1999, *ApJ*, 513, 656
- Dermer, C. D., & Chiang, J. 1999, in "GeV to TeV Gamma-Ray Astrophysics," *AIP Conf. Proc.* 515, eds. B. L. Dingus et al. (AIP: New York), 225
- Dermer, C. D., & Gehrels, N. 1995, *ApJ*, 447, 103; erratum 456, 412
- Dermer, C. D., Schlickeiser, R., & Mastichiadis, A. 1992, *A&A*, 256, L27
- Digel, S. W., Hunter, S. D., & Mukherjee, R. 1995, *ApJ*, 441, 270
- Digel, S. W., et al. 1996, *ApJ*, 463, 609
- Digel, S. W., et al. 1999, *ApJ*, 520, 196
- Dingus, B. L., Catelli, J. R., & Schneid, E. J. 1997, *Proc. 25th ICRC (Durban)*, 3, 29
- Dingus, B. L., Catelli, J. R., & Schneid, E. J. 1998, in *Proc. 4th Huntsville GRB Symposium*, *AIP Conf Proc*, 428, 349
- Drury, L. O'C., Aharonian, F. A., & Völk, H. J. 1994, *A&A*, 287, 959
- Espinoza, J. A., et al. 1996, *ApJ*, 461, 820
- Fenimore, E. E., Ramirez-Ruiz, E., & Wu, B. 1999, *ApJ*, 518, L73
- Fenimore, E. E., & Ramirez-Ruiz, E. 2000, *astro-ph/0004176*
- Fishman, G. J., & Meegan, C. A. 1995, *ARA&A*, 33, 415
- Forman, M., Ramaty, R., & Zweibel, E. 1986, in *Physics of the Sun*, ed. P. Sturrock et al., vol II (Dordrecht: Reidel), 249
- Fossati, G., Maraschi, L., Celotti, A., Comastri, A., & Ghisellini, G. 1998, *MNRAS*, 299, 433
- Fryer, C. L., Woosley, S. E., & Hartmann, D. H. 1999, *ApJ*, 526, 152F
- Gaidos, J. A. et al. 1996, *Nature*, 383, 319
- Gaisser, T. K., Halzen, F., & Stanev, T. 1995, *Phys. Reports*, 258(3), 173
- Gehrels, N., et al. 2000, *Nature*, 404, 363
- Ghisellini, G., & Madau, P. 1996, *MNRAS*, 280, 67
- Goldberg, H. 1983, *Phys. Rev. Lett.* 50, 1419
- Green, A. J., et al. 1997, *AJ*, 114, 2058
- Green, D. A. 1998, "A Catalog of Galactic Supernova Remnants." Available at <http://www.mrao.cam.ac.uk/surveys/snrs/>
- Grenier, I. A. 1999, in *Proc. 19th Texas Symposium on Relativistic Astrophysics and Cosmology*, ed. J. Paul, T. Montmerle, & E. Aubourg, in press
- Halpern, J. P., & Holt, S. S. 1992, *Nature*, 357, 222
- Harding, A. K. 1981, *ApJ*, 245, 267
- Harding, A. K., & Zhang, B., 2000, *ApJ*, submitted
- Hartman, R. C., et al. 1992, *ApJ*, 385, L1
- Hartman, R. C., et al. 1997, in the *Proc. of the Fourth Compton Symposium*, ed. C. D. Dermer, M. S. Strickman, & J. D. Kurfess (New York: AIP), 307
- Hartman, R. C., et al. 1999, *ApJS*, 123, 79
- Heckler, A. F. 1997, *Phys. Rev. D*, 55, 480
- Higgs, L. A., Landecker, T. L., & Roger, R. S. 1977, *AJ*, 82, 718
- Hua, X., & Lingenfelter, R. 1987, *Sol. Phys.*, 107, 351
- Hunter, S. D., et al. 1994, *ApJ*, 436, 216
- Hunter, S. D., et al. 1997, *ApJ*, 481, 205
- Hurley, K., et al. 1994, *Nature*, 372, 652

- Johnson, W. N., et al. 1997, in the Proc. of the Fourth Compton Symposium, ed. C. D. Dermer, M. S. Strickman, & J. D. Kurfess (New York: AIP), 283
- Jones, B. B. 1998, Ph. D. thesis, Stanford Univ.
- Jungman, G., Kamionkowski, M., & Griest, K. 1996, Phys. Reports, 267, 195
- Kamionkowski, M. 1995, in The Gamma Ray Sky with CGRO and SIGMA, ed. M. Signore, P. Salati, & G. Vedrenne (Dordrecht: Kluwer Academic Publishers), 113
- Kamionkowski, M., & Spergel, D. N. 1994, ApJ, 432, 7
- Kanbach, G., et al. 1993, A&AS, 97, 349
- Kaul, R. K., & Mitra, A. K. 1997, Proc. 4th Compton Symposium, ed. C. D. Dermer, M. S. Strickman, & J. D. Kurfess (New York: AIP), 1271
- Kohnle, A., et al. 1999, Proc. 26th ICRC (Salt Lake City), 5, 239
- Königl, A. 1981, ApJ, 243, 700
- Koratkar, A., Pian, E., Urry, C. M., & Pesce, J. E. 1998, ApJ, 492, 173
- Kouveliotou, C., et al. 1998, Nature, 393, 235
- Koyama, K., et al. 1995, Nature, 378, 255
- Kribs, G. D., & Rothstein, I. Z. 1997, Phys. Rev. D, 55, 4435; Erratum Phys. Rev. D, 56, 1822
- Kubo, H., et al. 1998, ApJ, 504, 693
- Lagage, P. O., & Cesarsky, C. J. 1983, A&A, 125, 249
- Lamb, D. Q., & Reichart, D. E. 2000, ApJ, 536, 1
- Lingenfelter, R. E. 1992, in The Astronomy and Astrophysics Encyclopedia, ed. S. P. Maran (New York: Van Nostrand Reinhold)
- Lundgren, S. C., et al. 1995, IAU Circular 6258
- MacMinn, D., & Primack, J. R. 1996, Space Science Reviews, 75, 413
- Macomb, D. et al. 1995, ApJ 449, L99
- Mandzhavidze, N., & Ramaty, R. 1992a, ApJ, 389, 739
- Mandzhavidze, N., & Ramaty, R. 1992b, ApJ, 396, L111
- Mannheim, K., & Biermann, P. L. 1992, A&A, 253, L21
- Maraschi, L., et al. 1993, ApJ, 435, L91
- Maraschi, L., Ghisellini, G., & Celotti, A. 1992, ApJ, 397, L5
- Marscher, A. P. 1996, in ASP Conference Series 100: Energy Transport in Radio Galaxies and Quasars, ed. P. E. Hardee, A. H. Bridle, J. A. Zensus, 45
- Marscher, A. P., & Bloom, S. D. 1994, in The Second Compton Symposium, ed. C. E. Fichtel, N. Gehrels & J. P. Norris (New York: AIP), 573
- Martinez, R., et al. 1999, Proc. 26th ICRC (Salt Lake City), 5, 219
- Mattox, J. R., et al. 1996, A&AS, 120, 95
- Mattox, J. R., et al. 1997, ApJ, 476, 692
- Mayer-Hasselwander, H. A., et al. 1998, A&A, 335, 161
- McLaughlin, M. A., et al. 1996, ApJ, 473, 763
- McLaughlin, M. A., & Cordes, J. M. 2000, ApJ, 538, 818
- Meegan, C. A., et al. 1992, Nature, 355, 143
- Meszáros, P., & Rees, M. J. 1997, ApJ, 476, 232M
- Metzger, M. R., et al. 1997, Nature, 387, 879
- Meyer, P. 1969, ARA&A, 7, 1
- Mirabal, N. & Halpern, J. P. 2001, ApJ Letters in press
- Morganti, R., et al. 1992, MNRAS, 256, 1P
- Mori, M. 1997, ApJ, 478, 225
- Mori, M., et al. 2000, Proc. International Symposium on High Energy Gamma-Ray Astronomy (Heidelberg), in press
- Mücke, A., & Pohl, M. 2000, MNRAS, 312, 177
- Mukherjee, R., et al. 1997, ApJ, 490, 116
- Navarro, J. F., Frenk, C., & White, S. D. M. 1996, ApJ, 462, 563, referred to as NFW in text
- Norris J. P., & Bonnell, J. T. 1999, in Proc. 19th Texas Symp. on Relativistic Astrophysics, in press
- Norris, J. P., Marani, G. F., & Bonnell, J. T. 2000, ApJ, 534, 248
- Oka, T., et al. 1999, ApJ, 526, 764
- Ong, R. 1998, Physics Reports, 305
- Ozel, M. E., & Thompson, D. J. 1996, ApJ, 463, 105
- Paczynski, B. 1998, ApJ, 494, L45
- Paredes, J. M., et al. 2000, Science, 288, 2340
- Parker, E. N. 1969, Sp. Sci. Rev., 9, 651
- Piran, T. 1999, Physics Reports, 314, 575
- Plaga, R. 1995, Nature, 374, 430
- Plaga, R., de Jager, O. C., & Dar, A. 1999, Proc. 26th ICRC (Salt Lake City), 4, 353
- Pohl, M., et al. 1997, ApJ, 491, 159
- Pohl, M., & Esposito, J. A. 1998, ApJ, 507, 327
- Primack, J. R., Bullock, J. S., Somerville, R. S., & MacMinn, D. 1999, Astropart. Phys., 11, 93
- Protheroe, R. J., & Biermann, P. L. 1997, Astropart. Phys., 6, 293
- Punsley, B. 1998, ApJ, 498, 640
- Quebert, J., et al. 1997, Proc. 25th ICRC (Durban), 5, 145
- Ramaty, R., & Murphy, R. 1987, Space Sci. Revs., 45, 213
- Ramirez-Ruiz, E., & Fenimore, E. E. 1999, ApJ, 539, 712
- Rees, M. J. 1984, ARA&A, 22, 471
- Rho, J. 1995, Ph.D. thesis., Univ. of Maryland, College Park
- Romani, R. W. 1996, ApJ, 470, 469
- Romero, G. E., Benaglia, P., & Torres, D. F. 1999, A&A, 348, 868
- Ryan, J., & Lee, M. 1991, ApJ, 368, 316
- Salamon, M. H., & Stecker, F. W. 1998, ApJ, 493, 547
- Salmonson, J. D. 2000, astro-ph/0005264
- Schneid, E. J., et al. 1993, in High Energy Solar Phenomena: A New Era of Spacecraft Measurements, ed. J. Ryan & T. Vestrand (Waterville, NH), AIP Conf. Proc., 294, 94
- Sikora, M., Begelman, M. C., & Rees, M. J. 1994, ApJ, 421, 153
- Sikora, M., & Madejski, G. 2000, ApJ, 534, 109
- Sreekumar, P. 1999, priv. comm.
- Sreekumar, P., et al. 1992, ApJ, 400, L67
- Sreekumar, P., et al. 1998, ApJ 494, 523
- Sreekumar, P., et al. 1999, APh, 11, 221
- Stecker, F. W., de Jager, O. C., & Salamon, M. H. 1992, ApJ, 390, L49
- Stecker, F. W., de Jager, O. C., & Salamon, M. H. 1996, ApJ, 473, L75
- Stecker, F. W., & Salamon, M. H. 1996, ApJ 464, 600
- Swanenburg, B. N., et al. 1978, Nature 275, 298

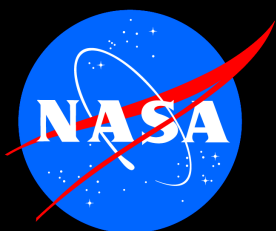
- Takahashi, T. et al. 1996, ApJ, 470, L89
 Takahashi, T. et al. 2000, ApJ, 542, L105
 Tanimori, T., et al. 1998, ApJ, 497, L25
 Tavani, M., et al. 1997, ApJ, 477, 439
 Tavani, M., et al. 1998, ApJ, 497, 89
 Thompson, D. J., & Fichtel, C. E. 1982, A&A 109, 352
 Thompson, D. J., et al. 1999, ApJ, 516, 297
 Tompkins, W. 1999, Ph.D. thesis, Stanford Univ.
 Totani, T. 1998, ApJ, 502, L131
 Totani, T., & Kitayama, T. 2001, ApJ, in press
 Trimble, V. 1989, ARA&A 25, 425
 Ullio, P., & Bergström, L. 1998, Phys. Rev. D57, 1962
 Ulrich, M.-H., Maraschi, L., & Urry, C. M. 1997, ARAA, 35, 445
 Urry, C. M., & Padovani, P. 1995, PASP, 107(715), 803
 van Paradijs, J., Kouveliotou, C., & Wijers, R. A. M. J. 2000, ARA&A, 38, 379
 Vasisht, G., & Gotthelf, E. V. 1997, ApJ, 486, L129
 Vermeulen, R. C., & Cohen, M. H. 1994, ApJ, 430, 467
 Vestrand, W., et al. 1997, ApJ, 483, 49
 von Montigny, C., et al. 1995, ApJ 440, 525
 Walker, K. C., Shaefer, B. E., & Fenimore, E. E. 2000, ApJ, 537, 264
 Waxman, E. 1995, Phys. Rev. Lett., 75, 386
 Wehrle, A. E., et al. 1998, ApJ, 497, 178
 Weinberg, S. 1983, Phys. Rev. Lett., 50, 387
 Willis, T. 1996, Ph.D. thesis, Stanford Univ.
 Yadigaroglu, I.-A., & Romani, R. W. 1995, ApJ, 449, 211
 Yadigaroglu, I.-A., & Romani, R. W. 1997, ApJ, 476, 347
 Yamasaki, N. Y., et al. 1997, ApJ, 481, 821

Figure Credits

- 2-1 EGRET instrument team/S. Digel
 2-2 GLAST project office/M. Fenske
 3-1 M. Catanese/A. Wehrle/Whipple Collaboration
 3-2 D. Bertsch/C. Dermer/J. Mattox
 3-3 NOAO/J. Burns/D. Clarke/C. Dermer
 3-4 S. Digel
 3-5 S. Digel
 4-1 EGRET instrument team/L. McDonald
 4-2 S. Digel
 4-3 S. Digel
 5-1 T. Willis
 5-2 G. Kribs/I. Rothstein
 6-1 C. Dermer
 6-2 J. Bonnell/J. Norris
 6-3 B. Dingus
 6-4 J. Bonnell
 6-5 GBM Collaboration
 7-1 D. Thompson
 7-2 R. Romani
 7-3 A. Harding/R. Romani/D. Thompson
 7-4 A. Harding
 8-1 S. Hunter
 8-2 S. Digel
 8-3 S. Digel
 8-4 P. Sreekumar/S. Digel
 8-5 C. Madsen/S. Digel
 8-6 S. Digel
 9-1 D. Bertsch
 9-2 G. Kanbach/J. Myers
 9-3 IPS Radio and Space Services/S. Digel
 10-1 Whipple Collaboration/T. Weekes
 11-1 S. Ritz
 11-2 LAT Collaboration
 11-3 GBM Collaboration
 12-1 GLAST Project Office/L. Londot

Contributors to this Document

- Glenn Allen (MIT)
 Matthew Baring (Rice Univ.)
 David Bertsch (GSFC)
 Elliott Bloom (SLAC)
 Jerry Bonnell (GSFC/USRA)
 Lynn Cominsky (Sonoma State Univ.)
 Charles Dermer (NRL)
 Seth Digel (GSFC/USRA; editor)
 Brenda Dingus (Univ. of Wisconsin)
 Gerald Fishman (MSFC)
 Neil Gehrels (GSFC)
 Alice Harding (GSFC)
 Robert Hartman (GSFC)
 Marc Kamionkowski (Caltech)
 Scott Lambros (GSFC)
 Peter Leonard (GSFC/Raytheon ITSS)
 John Mattox (Francis Marion Univ.)
 Charles Meegan (MSFC)
 Peter Michelson (Stanford Univ.)
 John Myers (GSFC/SP Systems)
 Jay Norris (GSFC)
 Jonathan Ormes (GSFC)
 Martin Pohl (Ruhr-Universität Bochum)
 Steven Ritz (GSFC)
 Roger Romani (Stanford Univ.)
 James Ryan (Univ. of New Hampshire)
 Floyd Stecker (GSFC)
 David Thompson (GSFC)
 Stephen Thorsett (UCSC)
 Trevor Weekes (SAO)



<http://glast.gsfc.nasa.gov>

December 2000

